An-Najah National University

Faculty of Graduate Studies

Bio-Functionalization of SWCNTs with Combretastatin A4 for Targeted Cancer Therapy

By

Deema Fahim Hamad

Supervisors

Dr. Mohyeddin Assali

Co-Supervisors

Prof. Abdel Naser Zaid

This Thesis is Submitted in Partial Fulfillment of the Requirement for the Degree of Master of Pharmaceutical Sciences, Faculty of Graduate Studies, An-Najah National University, Nablus- Palestine.

2017

Bio-Functionalization of SWCNTs with Combretastatin A4 for Targeted Cancer Therapy

By

Deema Fahim Hamad

This Thesis was defended successfully on 25/5/2017 and approved by:

Defense Committee Members	**Signature**
1. Dr. Mohyeddin Assali / Supervisor	**.....**
2 Prof. Dr. Abdel Naser Zaid/co-Supervisor	**.....**
3. Dr. Hatem Hejaz / External Examiner	**.....**
4. Dr. Aymen Hussein / Internal Examiner	**.....**

Dedication

To the most affectionate father in the world who is supporting and encouraging me throughout my life.

To the greatest mother who is carrying my burdens, tiring on me, forgiving my mistakes and standing beside me until became what I am now.

To my Sisters Wala' and Raghad and my brothers Rushdi and Hisham.

To my elder sister Nagham, her husband Anas and their beautiful children: Maher and Sana.

To My grandparents and my big family.

To every friend, I knew stood beside me and supported me

I dedicate this work

Acknowledgement

First of all, I thank the holy god for giving me the ability, qualifications and the patience to accomplish this research and be proud of myself.

Then, I want to express from my heart my deepest gratitude and thanks to my thesis supervisors: Dr. Mohyeddin Assali for all his support, help, guidance and sound advice in all portion of my research work and Prof. Dr. Abdel Naser Zaid for his scientific support and constructive advice.

Special thanks to Dr. Naim Kittana and Dr. Johnny Amer for assist, help and their guidance in the *in vitro* and cancer tests.

I would like to thank the rest of examination committee, for reading my thesis, their insightful comments and suggestions, and invaluable criticisms.

Thanks to Hamdi Mango Center for Scientific Research, Faculty of Medicine and Faculty of Science at the University of Jordan for their collaboration in SEM, TEM and TGA measurements.

Special and deepest thanks to the staff of the laboratories of the College of Pharmacy, Science and Medicine for providing help and assistance, especially the supervisor of the laboratories of the College of Pharmacy Mr. Mohammad Arar and the lab workers Tahrrer Ishtayeh and Linda Arar.

My friends and colleagues in the Department of Pharmacy deserve warm thanks, for their assistance, support and the most beautiful fun time that we spend it together during the period of my study.

My family, which doesn’t have any words to express my love, thanks and gratitude to them for their psychological and moral support throughout the years of my studies and work in my research. I hope you will be proud of me.

Deema Hamad

الإقرار

أنا الموقعة أدناه موقع الرسالة التي تحمل العنوان:

التفعيل البيولوجي لأنابيب الكربون النانونية بمركب كومبريتاستاتين أ4 لعلاج السرطان بطريقة مستهدفة

أقر بأن ما اشتملت عليه الرسالة هو نتاج جهدي الخاص، باستثناء ما تمت الإشارة إليه حيثما ورد، وأن هذه الرسالة ككل، أو أي جزء منها لم يقدم من قبل لنيل أي درجة أو لقب علمي أو بحثي لدى أي مؤسسة تعليمية أو بحثية أخرى.

Declaration

The work provide in this thesis, unless otherwise referenced, is the researcher's own work, and has not been submitted elsewhere for any other degree or qualification.

اسم الطالبة: **Student's name:**

التوقيع: **Signature:**

التاريخ: **Date:**

Table of contents

List of Figures

List of Schemes

List of abbreviations

Symbol	Abbreviation
$(C_2H_5)_2O$	Diethyl ether
1,2-DCB	1,2-Dichlorobenzene
^{99m}Tc	Technetium-99
Anhydrous $CuSO_4$	Anhydrous copper sulfate
Arg	Arginine
Asp	Asparagine
Boc_2O	Di-tert-butyl-dicarbonate
C_3H_8O	Isopropyl alcohol
CA4P	Combretastatin A4 phosphate
$CDCl_3$	Deuterochloroform
CGM	Culture growth medium
CH_3CN	Acetonitrile
$CHCl_3$	Chloroform
CNTs	Carbon nanotubes
CO_2	Carbon dioxide
Combretastatin	CA4
cRGDyK	Ligand of integrin
CVD	Chemical vapor deposition
DCM	Dichloromethane
DDs	Drug delivery systems
DIPEA	Diisopropylethylamine
DMAP	4-Dimethylaminopyridine
DMEM	Dulbecco's Modified Eagle's Medium
DMF	Dimethylformamide
DNA	Deoxyribonucleic acid

DOX	Doxorubicin
EAD	Electric arc-discharge
EDC	Ethylcarbodiimide hydrochloride
EPR	Enhanced permeability and retention
Et_3N	Trimethylamine
EtOAc	Ethylacetate
FA	Folic acid
FBS	Fetal bovine serum
f-MWCNTs	Functionalized multi-walled Carbon Nanotube
f-SWCNTs	Functionalized single-walled Carbon Nanotube
GPa	Gigapascal
H	Hour or Hours
H_2	Hydrogen gas
H_2O	Water
H_2SO_4	Sulfuric acid
Hcl	Hydrochloride
Hex	Hexane
HPLC	High Performance Liquid Chromatography
HUVECs	umbilical vein endothelial cells
IL-1β	interleukin 1β
KCN	Potassium cyanide
LA	Laser ablation
LCL	Long circulating liposomes
L-Glu	L-glutamine
MeOH	Methanol
Min	Minutes

MsCl	Mesyl chloride
MTX	Methotrexate
MW	Molecular weight
MWCNT	Multi-walled carbon nanotube
Na_2SO_4	Sodium sulfate
NaCl	Sodium chloride
NaH	Sodium hydride
$NaHCO_3$	Sodium bicarbonate
NaN_3	Sodium azide
NaOH	Sodium Hydroxide
NaOH	Sodium Hydroxide
NMR	Nuclear Magnetic Resonance
^{o}C	Celsius
o-DCB	Ortho dicholrobenzene
PBS	Phosphate buffer saline
Pd/C	Palladium on carbon
PEG	Polyethylene-glycol
Pen-Strep	Penicillin- streptomycin
pH	Power of hydrogen
PI	Propidium iodide
PLA	Poly lactic acid
p-SWCNTs	Pristine single-walled Carbon Nanotubes
Pt(IV)	Platinum(IV)
RBF	Round bottom flask
ROS	Reactive oxygen stress
Rpm	Round per minutes
RT	Room temperature
SEM	Scanning Electron Microscopy

siRNA	Short interference RNA
SO_3	Sulfur trioxide
SWCNT	Single-walled Carbon Nanotube
Tbf	Tetrabenzo fluorine
TBTU	2-(1H-Benzotriazole-1-yl)-1,1,3,3-tetramethyluronium tetrafluoroborate
TEG	Tetraethylene glycol
TEM	Transmission electron microscope
TFA	Trifluoroacetic acid
TGA	Thermogravimetric analysis
THF	Tetrahydrofuran
TLC	Thin layer chromatography
Tpa	Terapascal
URPA	Pullulan-based nanoparticle
UV-Vis	Ultraviolet-Visible
VDA	Vascular distrusting agent
WHO	World Health Organization
λ_{max}	Lambda max

Bio-Functionalization of SWCNTs with Combretastatin A4 for Targeted Cancer Therapy

By
Deema Fahim Hamad
Supervisors
Dr. Mohyeddin Assali
Co-Supervisors
Prof. Abdel Naser Zaid

Abstract

Chemotherapy is a mainstay approach in the management of cancer. Unfortunately, it can affect not only the cancerous cells but also the healthy ones resulting in a number of severe side effects. Therefore, many researchers are keen to developing new Drug Delivery Systems (DDS) that may in one hand help reducing the used doses and on the other hand target the delivery of the chemotherapy to cancer cells. Some modern investigational DDS in this field are based on carbon nanotubes (CNTs) technology.

The aim of this work is to covalently functionalize single walled carbon nanotubes (SWCNTs) with Combretastatin A4 (CA4) through click reaction in the presence of tetraethylene glycol linker to improve the solubility and dispersibility of the developed nano-drug. Moreover, in order to specifically target the cancer cells, a targeting agent folic acid was also loaded on the nano-system. The characterization of the developed nano-drug by scanning electron microscopy (SEM) and transmission electron microscopy (TEM) showed good dispersibility of the functionalized SWCNTs with diameters of (5-15) nm. Moreover, the efficiency of functionalization was determined by thermogravometric analysis (TGA)

showing 45% of functionalization in the case of CA4-SWCNTs **(7)** and 50% for CA4-FA-SWCNTs **(13)**. The *in vitro* release profile of CA4 showed that approximately 90% of the loaded drug was released over 50 hrs at pH 7.4 and 37 ºC.

MTS proliferation test was implemented to determine the suitable concentration for the CA4-SWCNTs **(7)**, which was found to be 15 ng/ml. After that the cytotoxic activity of the nano-drug was evaluated by flow cytometry using Annexin V/Propidium iodide (PI) test. In comparison with free CA4, CA4-SWCNTs **(7)** treatment demonstrated a significant increase in necrotic cells (around 50%) at the expense of the proportion of the apoptotic cells. Moreover, cell cycle PI test demonstrated that free CA4 and CA4-SWCNTs **(7)** caused G2/M arrest. However with CA4 treatment higher proportion of cells were in the S-phase while with CA4-SWCNTs treatment greater proportion of cells appeared to be in the G1-phase. Taken together, the provided data suggest that the novel CA4-SWCNTs **(7)** has a significant anticancer activity that might be superior to that of free CA4. The anticancer activity of CA4-FA-SWCNTs **(13)** is under investigation.

Chapter One
Introduction

1.1. Cancer

Cancer is defined as disease that begins when a normal cell (or group of cells) is converting to abnormal cell through multistage process because of DNA mutation (genetically from parents or due to external carcinogens). The cell is unable to correct damaged DNA and unable to suicide leading to uncontrollable cell growth (Figure 1.1) [1, 2].

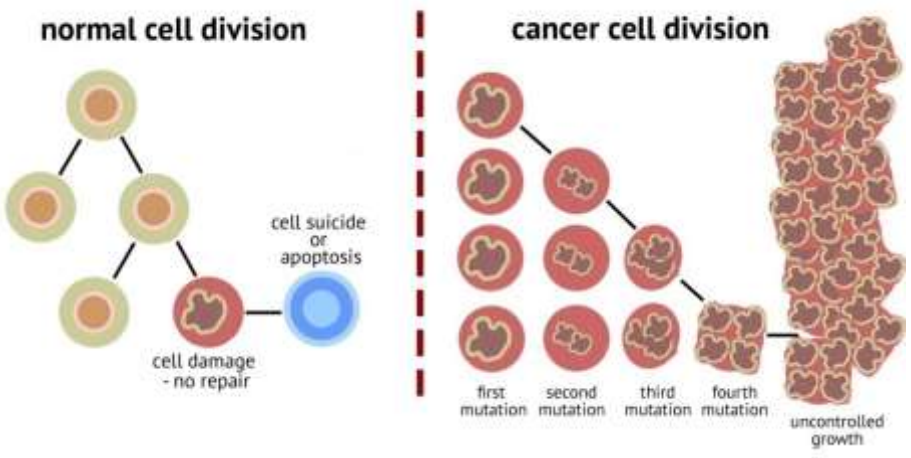

Figure 1.1: Difference between normal cell division (Left) and uncontrollable growth of cancer cell (Right) [2].

Moreover, tumor cells are able to grow beyond their usual boundaries and invade neighbor tissues in process called “Metastasis” (Figure1.2 A). Also, it builds up their own blood vessels in a process called “Angiogenesis” (Figure 1.2 B) [3, 4]. Moreover, it can stimulate the neighbor normal cells to produce angiogenic factors which increase the production of new blood vessels which are required to respond the high demand of oxygen and nutrients [5, 6].

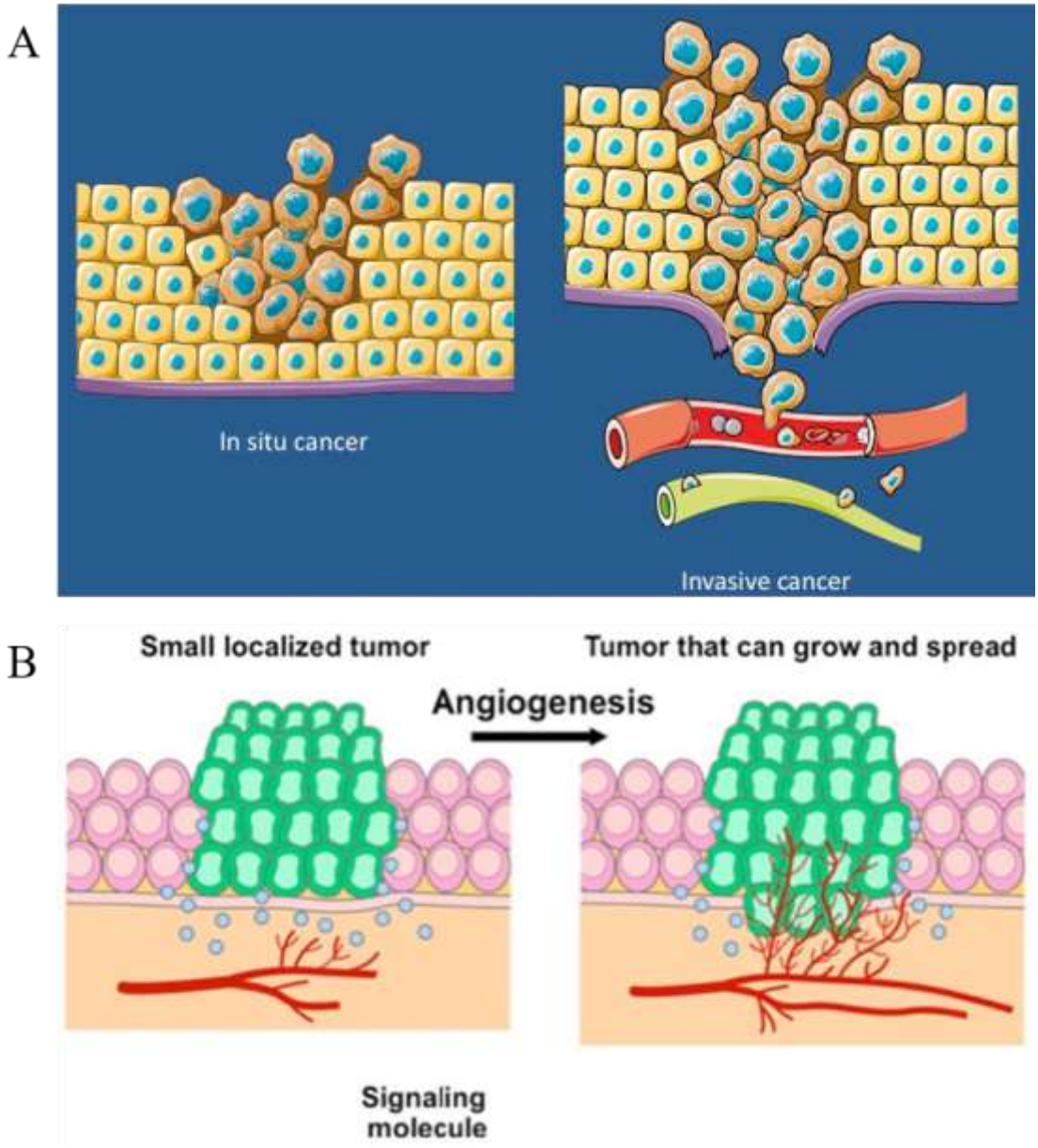

Figure1.2:(A) Type of cancer: a. in situ cancer b. invasive cancer[3]. **(B)** Angiogenesis of cancer cell [7].

In fact, these blood vessels that fed the tumor cells are different from normal cells [8]. They are immature, have loose structure, abnormal in the vascular wall, proliferate more rapidly and the endothelial cells lining are discontinuous [9, 10]. These differences were discovered by a Japanese scientist Maeda and was called enhanced permeability and retention (EPR) effect. This effect results in leakage of plasma blood component to the

tumor tissue including macromolecules causing an increase in the interstitial fluid pressure as shown in Figure 1.3 [11-13].

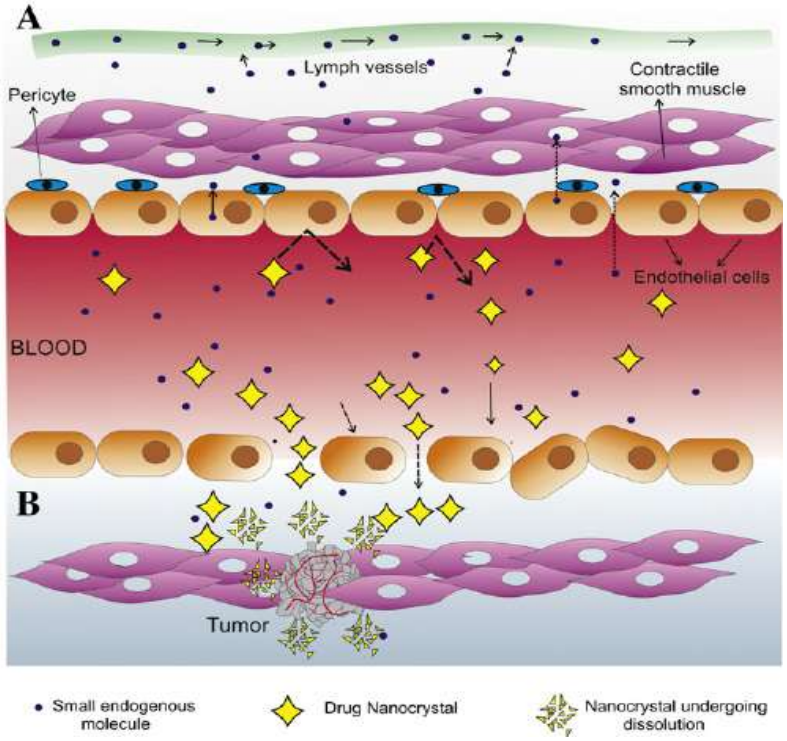

Figure 1.3: EPR effect; (A) endothelium of normal blood vessels permit only small molecules to penetrate **(B)** endothelium of tumor blood vessels permit macromolecules and small molecules penetrate to tumor cells**[13].**

In 2012, the last statics of WHO showed that 8.2 million of deaths occurred because of the cancer disease, 14 million new cases were reported and 32.6 million people were living with cancer. More than 60% of world's new cases occur in Africa, Asia, Central and South America. 70% of the world cancer deaths occurred in these regions. In addition, the annual cancer cases are expected to reach about 22 million by 2025 [14].

Among men, the five most common types of cancer that were diagnosed are: lung, prostate, colorectum, stomach and liver. Lung and prostate cancer had the highest incidence, respectively. Among women, the most common

types are: breast, colorectum, lung, cervix and stomach. Figure 4 show the percentage of cancer mortality according to the cancer disease type in both sex (Figure 1.4) [14].

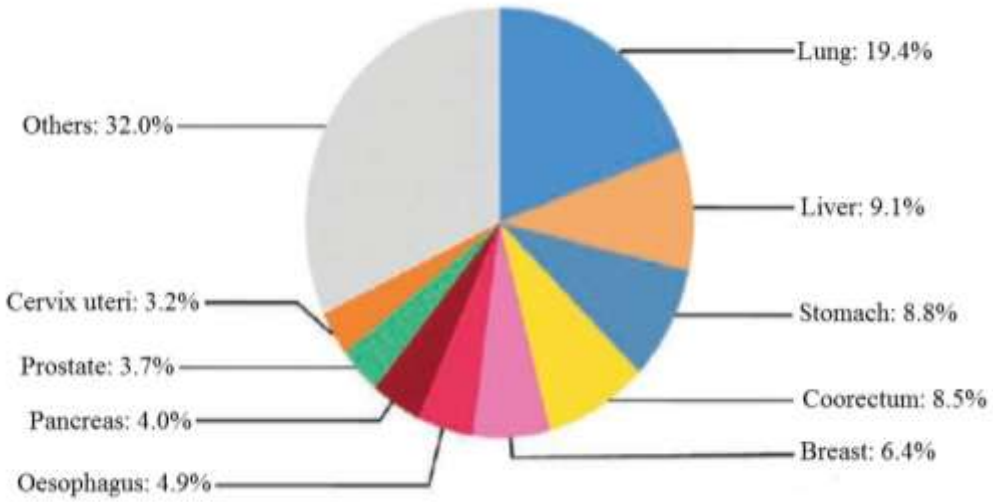

Figure1.4: The percentage of the cancer mortality according to the cancer disease type in both sex [14].

The used intervention strategies for cancer treatment are surgery, radiotherapy, chemotherapy, targeted therapy, immunotherapy, and other types of therapies [15-17]. Chemotherapy is the most common intervention that has been recently used. It is usually used to cure the cancer or decrease the symptoms and prevent the spreading of cancer. However, chemotherapy can cause serious side effects including damages of the nerves, deficiency in the immune system, bleeding, dry mouth, stomach upset, vomiting, diarrhea, and hair loss [18]. Recently, a novel interventional approach has been introduced to reduce these side effects. This method is based on nano-pharmaceutical technology such as nanoparticles and liposomes. These drug delivery systems (DDS) were

developed to deliver the chemotherapeutic drugs by taking advantage of EPR effect in the tumors.

Carbon nanotubes (CNTs) are considered one of the most interesting DDS that have been developed for specific targeting of anti-tumor drugs [19].

1.2. Carbon nanotubes (CNTs)

CNTs are allotropic form of carbon (Figure 1.5) [20]. They are nanomaterials which have needle like structure with large surface area. They were discovered by Japanese physicist Sumio Iijima in 1991 [21]. CNTs are described as sheets of six-membered carbon atom rings which are wrapped into cylindrical tube [22, 23].

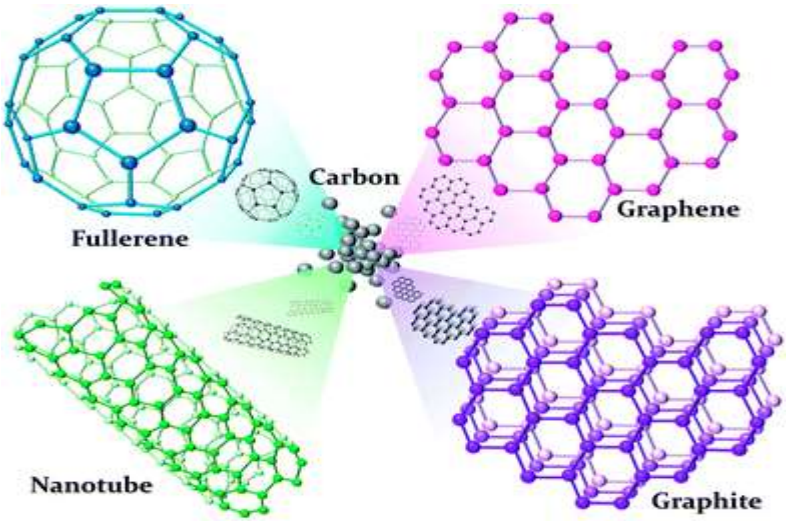

Figure1.5: Allotropes of carbon[20].

According to the number of layers that form the final nano-tubes, CNTs are classified into single-walled carbon nanotubes (SWCNTs) and multiple-walled carbon nanotubes (MWCNTs) (Figure 1.6) [24, 25]; MWCNTs was firstly discovered in 1991 and it consists of several layers of graphite sheets

with layer separation of 0.34 nm and diameter between (1-100nm) [21]. On the other hand, SWCNTs was discovered two years later and it consists of only one layer of graphite sheet (one cylinder), diameter between (0.4-3 nm) and the length-to-diameter ratio exceeds 10,000 [26].

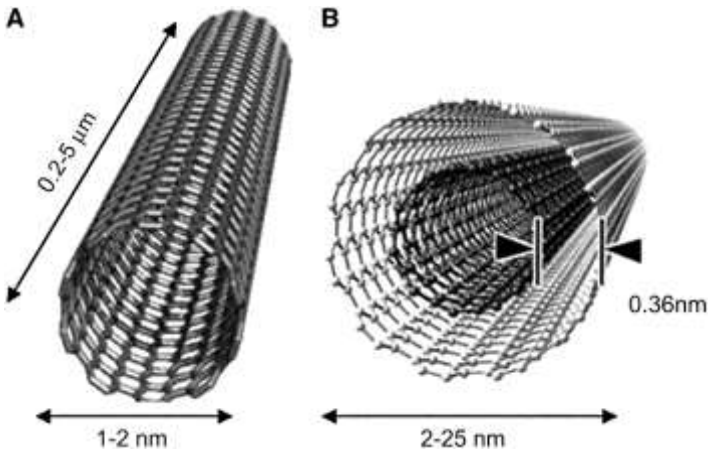

Figure 1.6: Classification of CNTs according to number of layer: A. SWCNTs B.MWCNTs [25].

CNTs are considered to be surprising materials of the 21st century because of their interesting electrical, optical and structural properties. In fact, CNTs exhibits fascinating properties such as:

- Electrical properties: CNTs could be either metals or semiconductors depending on structure and chiral vector [27]. Metallic nanotubes have an electrical current density about 1 billion A/cm^2 which is more than 1,000 times greater than copper wires. Accordingly, it have been used in different areas in nano-electronics including transistors, sensory devices and memories [28].

- Thermal properties: CNTs showed good thermal conductivity. In fact, the approximate temperature stability of CNTs is up to 2800 ^{o}C in vacuum, and

up to 750 ^{O}C in air. Furthermore, the heat transmission is expected to be as high as 6000 watts per meter per Kelvin at room temperature [28].

•Mechanical properties: CNTs demonstrated high tensile strength and elastic modulus. The elastic modulus value of a SWCNT is about 1Tpa to 1.8 Tpa [29]. In addition, the tensile strength of nanotubes are around 50 times higher than steel [30].

CNTs are applicable in many fields including electronics [31], biosensor technology [32], energy-storage devices [33]. However, CNTs have limited application in medicine because of their low solubility and high toxicity [34]. In fact, pristine CNTs (*p*-CNTs) may induce toxicity through several mechanism such as reactive oxidative stress (ROS) [35] and inflammatory responses [36].

Recently, it was found that the functionalization of CNTs would improve the water dispersibility of CNTs which could enhance the execration of CNTs from the body causing an increase in biocompatibility, and a decrease in their toxicity.

The *in vivo* toxicity of *f*-MWCNTs in mice was assessed by Guo*et al*. In this study, the MWCNTs were functionalized with glucosamine and then they were labeled with radioisotopes technetium-99 (^{99m}Tc-MWNT-G). The results shown that no severe acute toxicity responses were observed [37].

Functionalized SWCNTs using branched polyethylene-glycol (PEG) chains were injected intravenously to assess the biopharmaceutical behavior of the obtained functionalized nano-tubes. PEG increased the blood circulation of SWCNTs up to 1 day. In addition, these SWCNTs were detected in the intestine, feces, kidney, and bladder of mice. Moreover, the execration was via biliary and renal pathways. No toxic side effects of SWCNTs to mice were observed [35].

The pharmacokinetic and bio distribution of amino-SWCNTs were reported by McDevitt et al.[38, 39]. In this study the amino-SWCNTs remained in the body for more than 24 hours. After 3 hours, amino-SWCNTs accumulated in liver, spleen, kidneys and skin. Moreover, they assessed the capacity of amino-CNTs to deliver siRNA to tumor through intratumoral injection [40] and to brain through injection in the primary motor cortex [41].

1.3. Functionalization of CNTs

Generally, CNTs have low water dispersibility. In addition they also showed low dispersibility in most organic solvent due to their high tendency to aggregate by mean of their intermolecular forces [42, 43]. There are four types of functionalization are now available. The most common Types are covalent and noncovalent functionalization (Figure 1.7) [44]. Adding functional groups alongside the surface and on the defected sites of the nano-tubes would increase the water solubility, enhance the biocompatibility and consequently decrease their toxicity [45].

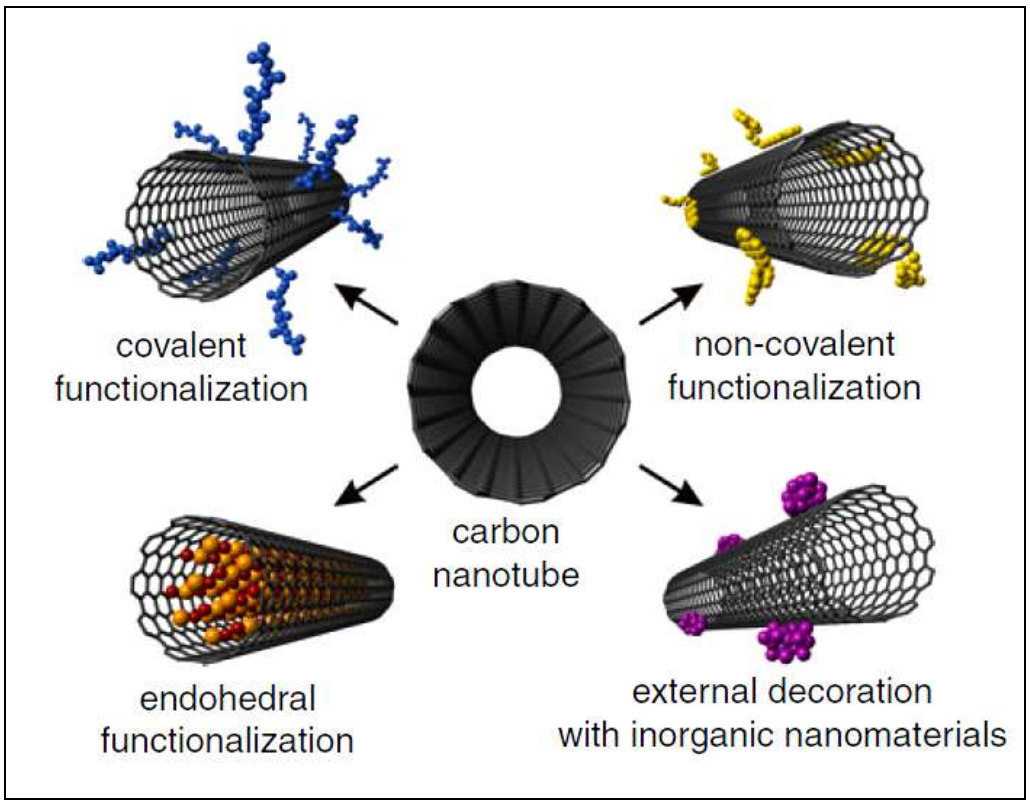

Figure 1.7: Schematic representation of different strategies for the functionalization of carbon nanotubes [44].

1.3.1. Non-covalent Functionalization

This type of functionalization occurs due to Vander Waals interaction between carbon nano-tubes and molecules. For example, aromatic compounds, polymers, and surfactants can be used to modulate the nano-tubes surface [46-48]. The obtained non-covalent functionalization maintains the electric properties of CNTs [49], but remain sensitive to environmental conditions such as pH and salt concentration. Accordingly, the release of the drugs that were charged on the surface of CNTs may occur before reaching the target site [49].

Therefore, using aromatic compounds which can interact with the surface of CNTs *via* π-π stacking interactions [50-52] was evaluated. In this

manner, Assali *et al.* have developed a new approach for increasing the biocompatibility of nanomaterials through non-covalent functionalization of the surface of CNTs with neoglycolipid compound by π–π stacking interactions (Figure 1.8) [53]. They synthesized neo-glyco-conjugates structure (compound I) which is a pyrene tail bonded to the glycol-ligand (sugar head) through as spacer, tetra ethylene glycol, which was employed for better hydrophilic/hydrophobic balance. These aggregates are able to attract specific ligand-lectin interactions similar to glycol conjugates on the cell membrane [53].

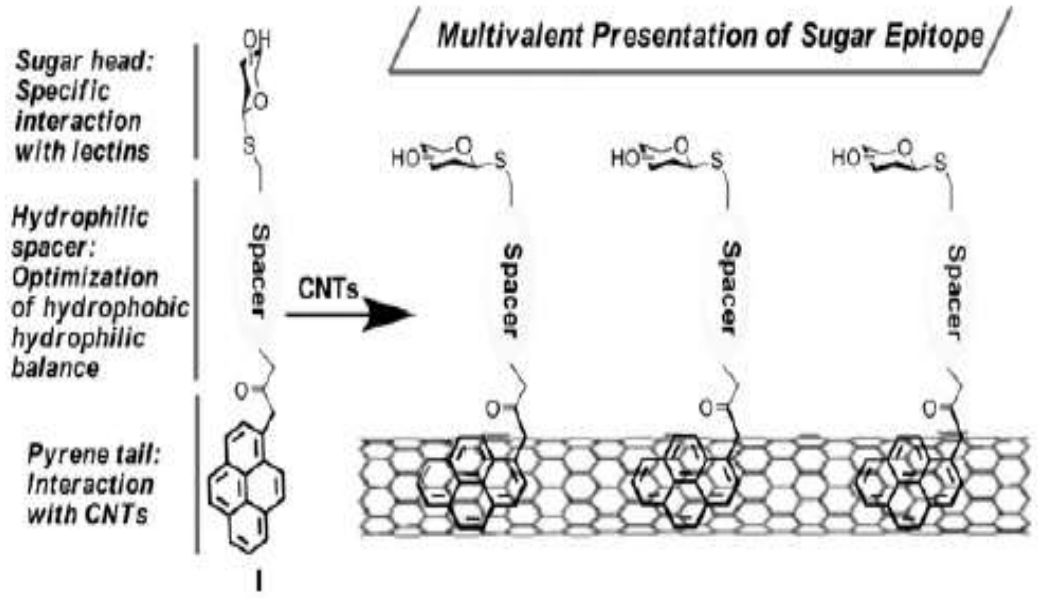

Figure1.8: Non covalent functionalization of CNTs with pyrene functionalized neoglycolipids [53].

In another study, Assali *et al.* have reported another non-covalent functionalization of MWCNTs with neogly-coconjugates. The strategy is based on the use of sugar-based amphiphiles functionalized with tetrabenzo[*a*,*c*,*g*,*i*]fluorine (Tbf), a polyaromatic compound with a topology that look like a butterfly with open wings (Figure 1.9). This system was

developed in order to improve the low ability of pyrene-based systems to exfoliate MWCNTs in water [54].

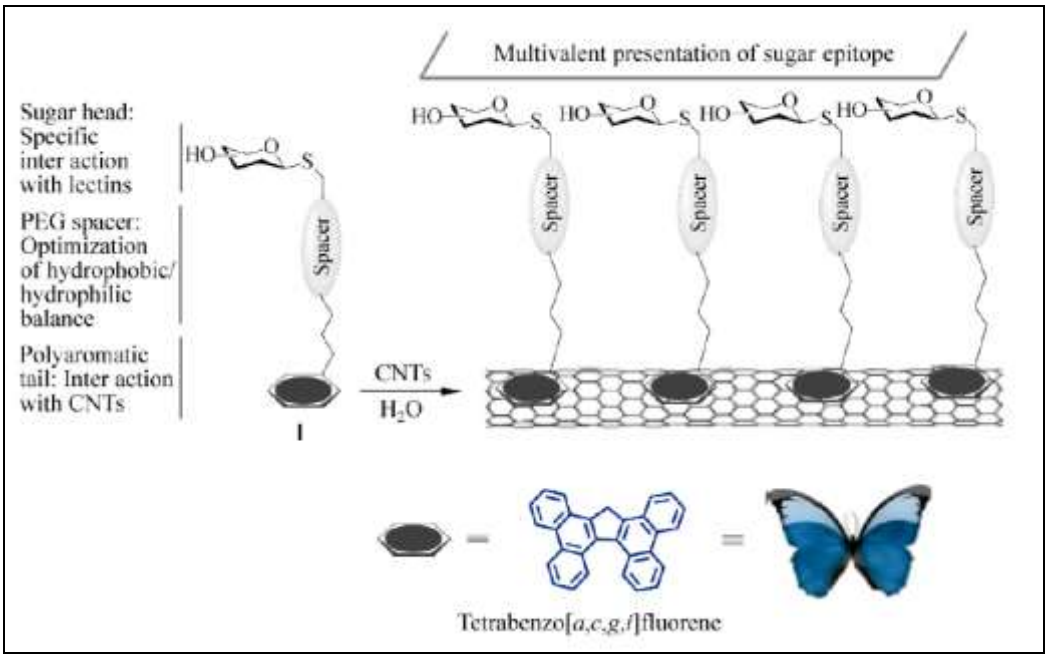

Figure 1.9: The synthesis of the Tbf-linked carbohydrate-MWCNTs[54].

1.3.2. Covalent functionalization

Covalent chemical modification can be achieved through oxidation reaction [55], arylation [56], addition reactions [57] and other reactions which involve other reactive species (Figure 1.10) [58]. Covalent functionalization changes the electrical properties of the CNTs as a result of change of carbon hybridization from sp^2 to sp^3 [19, 42, 59]. The aim of this type of functionalization is to prevent the release of the attached biomolecules before reaching the target site and consequently decreases the side effects of these biomolecules.

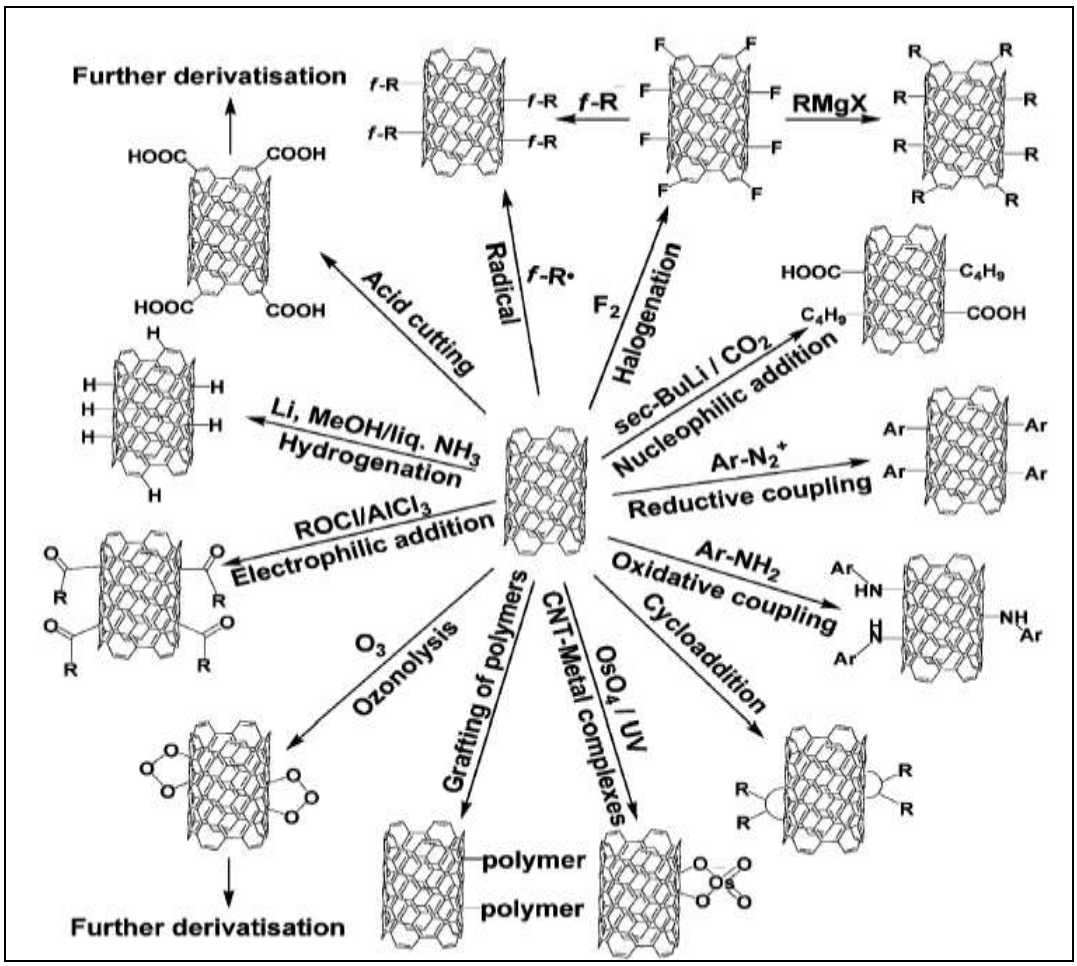

Figure 1.10: Covalent functionalization of carbon nanotubes [58].

1.3.2.1. Esterification or amidation of oxidized CNTs

Chen and co-workers reported the method for shortening and carboxylation of SWCNTs by dispersing the nano-tubes in oleum (concentrated H_2SO_4 with 3% SO_3), followed by adding a cutting agent (nitric acid). The inserted oleum between SWCNTs enhanced the activity of the cutting agent [60].

Carboxylate CNTs can be used to bind with wide range of molecules *via* amide and ester bond. This reactions occurs by converting the carboxyl group to the acyl chloride followed by an addition of alcohol or amine molecules (Figure 1.11) [61, 62].

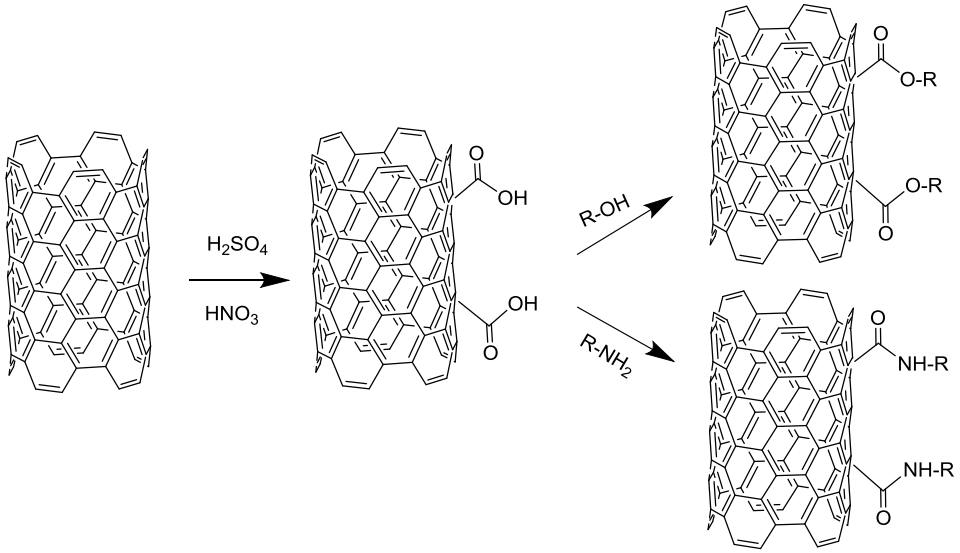

Figure 1.11: Esterification and amidation of oxidized CNTs [62].

1.3.2.2. Addition reactions

There are different types of addition reactions such as fluorination [63], addition of carbenes and nitrenes [64, 65], 1,3-dipolar cycloaddition [66, 67], Diels-Alder cycloaddition [68], nucleophilic additions [69], free-radical addition [70, 71] and electrophilic addition [72].

Tour and co-workers functionalized SWCNTs with reduced aryl diazonium salts *via* electrochemical reaction (Figure 1.12). The aryl radicals were generated from the diazonium salts by one-electron reduction and the buckypapers were used as working electrode [56]. After that, the obtained group reported the covalent sidewall modification of CNTs *via* in situ generated aryl diazonium salts from the conforming anilines. The obtained materials showed good-dispersibility in both organic and water solvents [73].

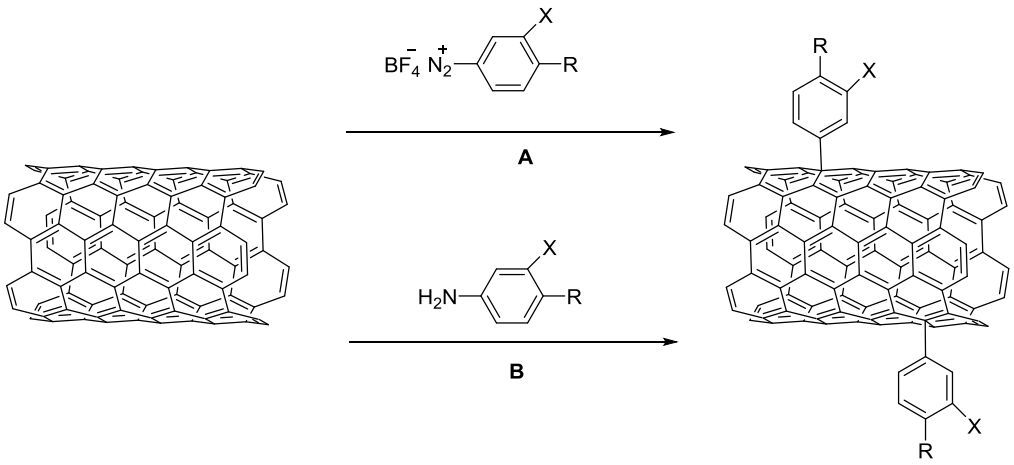

Fig 1.12: Functionalization of CNTs using diazonium coupling reactions under different conditions. A) In presence of surfactants or ionic liquids or electrochemical reaction. B) diazonium salt generated in situ with nitrites.

This research deals with a novel molecule of anti-cancer drug Combretastatin A4 (CA4) which has unique and specific mechanism of action on cancer cells. This drug targeted to specific tumor cell through covalent functionalization of SWCNTs.

1.4. Combretastatin A4 (CA4)

Combretastatin (CA4) is a vascular disrupting agent (VDA) which was extracted from African Cape Bush willow tree called *Combretum caffrum* [74, 75] . CA4 is tubulin binding agent which inhibits the polymerization of tubulin by self-attachment on colchicine or nearby binding receptor at the β-tubulin subunit [76, 77]. The depolymerization of tubulins activates microtubule associated proteins which activates the Rho associated protein kinase. Several effects on the endothelial cells are induced by RhoA kinase. These include increase in cell's detachment, increase stress fibers, disruption of cell/cell junctions, increase permeability and other effects which lead to cell apoptosis and vascular shutdown (Figure 1.13) [78-80].

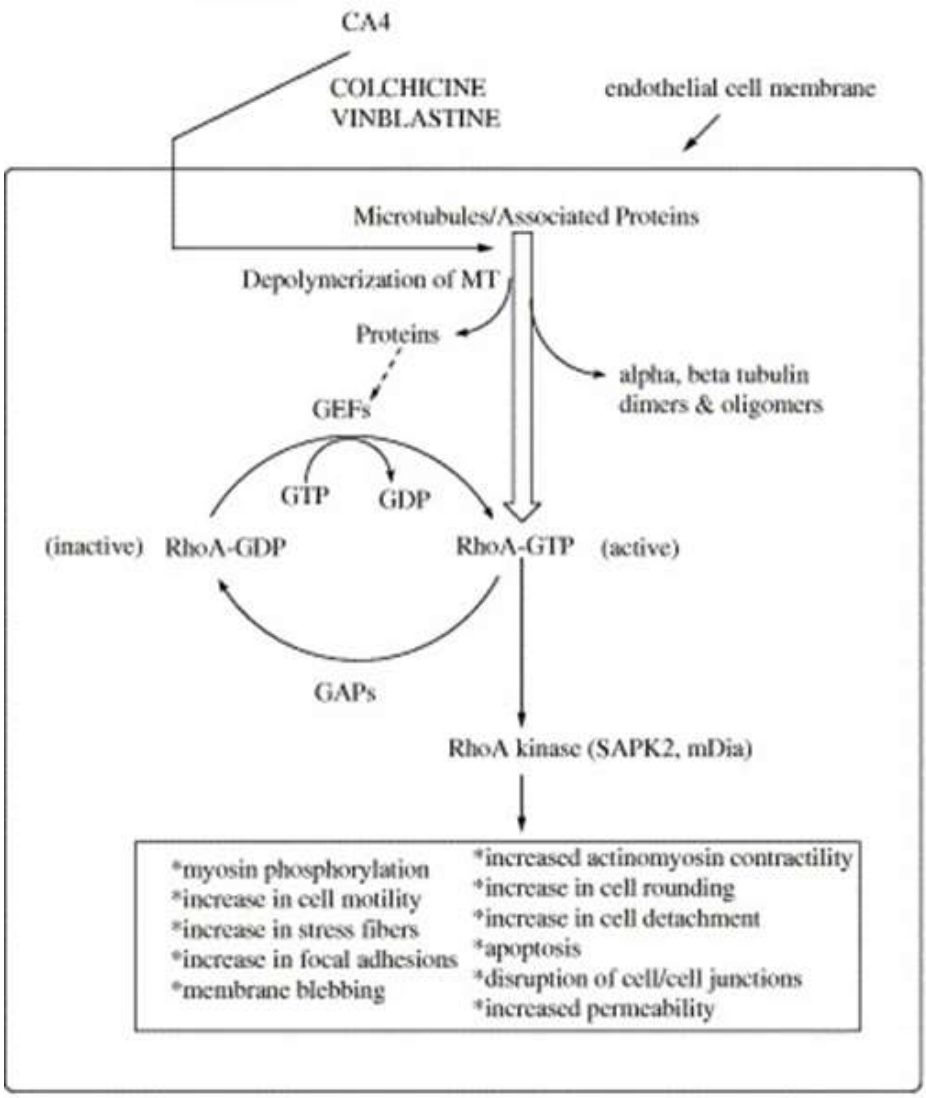

Figure1.13: Proposed mechanism of vascular disruption by tubulin-binding agents [78].

Moreover, it was demonstrated that CA4 not only disturb the tumor vascular system, but it also displays direct anti-angiogenic properties through inhibiting the migration of endothelial cells. Accordingly a prevention in the formation of new tumor blood vessels is occurred [81]. In addition, the metastasis could be achieved due to the inhibition of the migration and attachment of cancer cells to other sites of the body [82-85].

Chemically,CA4 is a 5-[(2R)-2-hydroxy-2-(3,4,5-trimethoxyphenyl)ethyl]-2-methoxyphenol with molecular weight 316.34 g\mol [86]. Two condensation methods (Wittig and Perkin) can be used to prepare the stilbene structure. In the Wittig reaction a mixture of the two geometrical isomers (*Z* and *E*) is always obtained. In the Perkin reaction, the *Z* isomer is predominated, but a high-temperature decarboxylation process is necessary to obtain the final product [87, 88]. The active geometrical isomer of CA4 is *Z* isomer (figure 1.14) [74]. Studies showed that the *Z* configuration is fundamental to have high cytotoxic and anti-tubulin action, while the *E* analogue is significantly less potent [89]. CA4 has a wide range therapeutic windows, it inhibits the tumor growth at doses up to ten folds less than the maximum tolerated dose [90, 91].

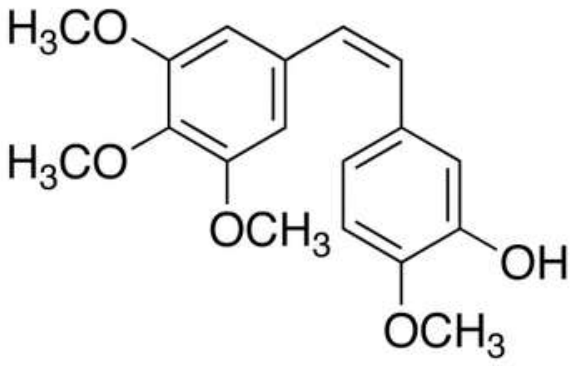

Figure1.14: Combretastatin A4 chemical structure [74].

The poor water solubility of CA4 led to the synthesis of water-soluble pro-drugs. The potassium and sodium phosphate derivatives of CA4 were found to be suitable, and the sodium phosphate derivative (CA4P) is selected for further preclinical development [92]. The structure and synthesis of CA4P were described in 1989. CA4P is clinically evaluated,

the results from the first phase I trials published in 2002 and 2003. The pro-drug undergoing phase II clinical evaluation in cancer patients [93, 94]. Fosbretabulin Disodium (Combretastatin A4 Phosphate (CA4P)) inhibits tubulin assembly with IC_{50} 2.4 μM [95]. According to the in vivo trials, the CA4P (100 mg/kg, 6 h following administration) reduce the blood flow by approximately 100-fold but the drug still in the clinical trials until now [96].

Inside cells, CA4P is converted to CA4 by endogenous non-specific phosphatases enzymes. The cytotoxicity profile for both the pro-drug and active compound are similar, indicating no loss of activity for CA4P [91].

Ombrabulin (AVE8062) is a CA4 derivative drug. In 2001, Sanofi Aventis have the agreement from Ajinomoto company to develop the drug. However, the development was discontinued in 2014 from Phase II\III because it didn't meet the primary objective of improving progression-free survival (PFS) in patients with metastatic non-small cell lung cancer (NSCLC) and other types of cancer, Figure 1.15 [97, 98].

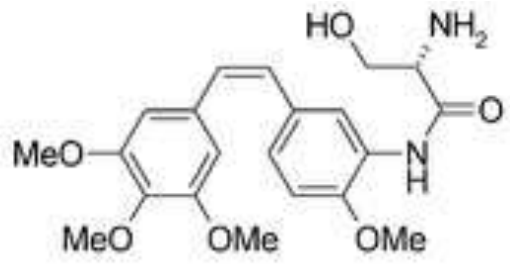

Figure 1.15: Ombrabulin chemical structure [99].

However, this is not the optimum approach for the application of CA4, because the distribution of the pro-drug in the body and the short half-

life (30 minutes) of the drug reduce its therapeutic efficacy and cause undesirable side effects in normal tissues, such as cardiotoxicity and ataxia [92].

To decrease the side effects and toxicity of CA4 a carrier system may be helpful in improving the water solubility, bioavailability and minimizing the side effects. Commonly drug delivery systems include liposomes [100, 101], polymeric nanoparticles and peptide conjugates [102, 103]. These drug delivery systems have been demonstrated to enhance the water solubility and improve the therapeutic efficacy of CA4 [100].

Herein, my project was conducted to develop a new nano anticancer product through the covalent functionalization of carbon nano-tubes using CA4 connected with a polyethylene glycol linker (PEG) in order to increase the water solubility and biocompatibility of the whole nano-system. Moreover, cancer cells over expresses folate receptors due to the high demand toward nutrients and rapid growth rate. Accordingly, in order to decrease the side effects on normal cells and increase the selectivity on the cancer cells, a specific targeting agent, (folic acid) was conjugated on the nano-system. [104, 105].

1.5. Literature Review

Many attempts were carried out in order to improve the efficacy and safety of the anticancer agents using different types of nano-systems such as nanoparticles, liposomes, micelles and others. In this literature review, Combretastatin A4 conjugated with nanomaterials were mainly reported.

In 2006, Nallamothu and co-workers developed long circulating liposomes (LCL) charged with CA4. These LCL were conjugated to the cyclic RGD (Arg-Gly-Asp) peptide, a targeting agent, to the HUVEC activated interleukin 1β (IL-1β) cell line. Approximately 80% of CA4 was loaded to LCL and the *in vitro* cytotoxic studies conducted on cancer cells showed that the targeted liposomes have higher association to the HUVEC (IL-1β) than normal HUVEC. In addition, the targeted liposomes showed improvement in the cytotoxicity of CA4 when compared to the non-targeted liposomes [101]. In another study, CA4 multifunctional dendrimers system were developed by Zhang et al [106]. The obtained dendrimers were partially acetylated on the terminal-amine of polyamidoamine dendrimers (G5) while the remaining terminal amines were attached to fluorescein isothiocyanate and folic acid as an imaging and targeting agents respectively. The *in vitro* studies showed that the inhibitory effect of these dendrimer complexes were similar to that of free CA4 at the same selected drug concentration. A selective targeting of these complexes, due to the over expression of folic acid receptors, was observed. [106]. One year later a dual-drug micelle system was developed by Yang *et al*. [107]. In this study, they attempted to conjugate doxorubicin (DOX) to the poly lactic acid (PLA) end of polyethylene glycol-b-poly lactic acid (PEG-b-PLA) while the targeting agent, a ligand of integrin, (cRGDyK) was conjugated to the PEG end. CA4 was linked to the PEG-b-PLA conjugates *via* solution-casting method. The results showed that the targeting dual-drug micelle system has antitumor, anti-proliferating and apoptosis effect on cancer cells [107]. In 2013, Wang and co-workers

developed a combinational therapy, based on pH-sensitive pullulan nanoparticle carrier containing methotrexate and CA4 – MTX/URPA conjugates (Figure1.16). The nano-particulate system intravenously injected to PLC/PRF/5 tumor-bearing nude mice. The results showed that the carrier system enhanced the antitumor activity, anti-angiogenic effect and regression of the tumor size in nude mice [108].

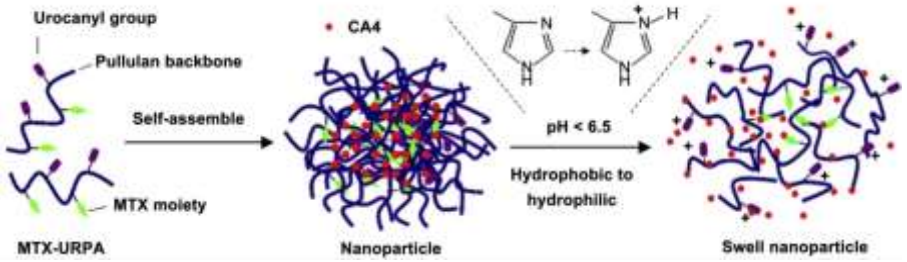

Figure1.16: Pullulan-based nanoparticle carrier contains methotrexate (MTX) and combretastatin (CA4) [108].

In 2014, Su *et al.* constructed two in one liposomal system (TWO lips). Approximately 96% of DOX and CA4 were loaded to the TWO lips. The developed liposomal system significantly inhibited tumor growth, and angiogenesis. In addition, enhanced survival of mice with melanoma xenografts was registered. Moreover, the drug-loaded system had a low potential risk of toxicity [109]. In 2016, Bolu *et al*. conjugated the CA4 to micelles using triblock Dendron-linear polymer. The system was fabricated by surrounding the polyethylene glycol (PEG) with biodegradable polymer Dendron bearing CA4 (Figure1.17). Different generations of dendron with varying sizes and drug loading were used in this study. The *in vitro* cytotoxicity was investigated on human umbilical vein endothelial cells

(HUVECs) and the results showed significant inhibitory effect of micelles system on these cancer cell line [110].

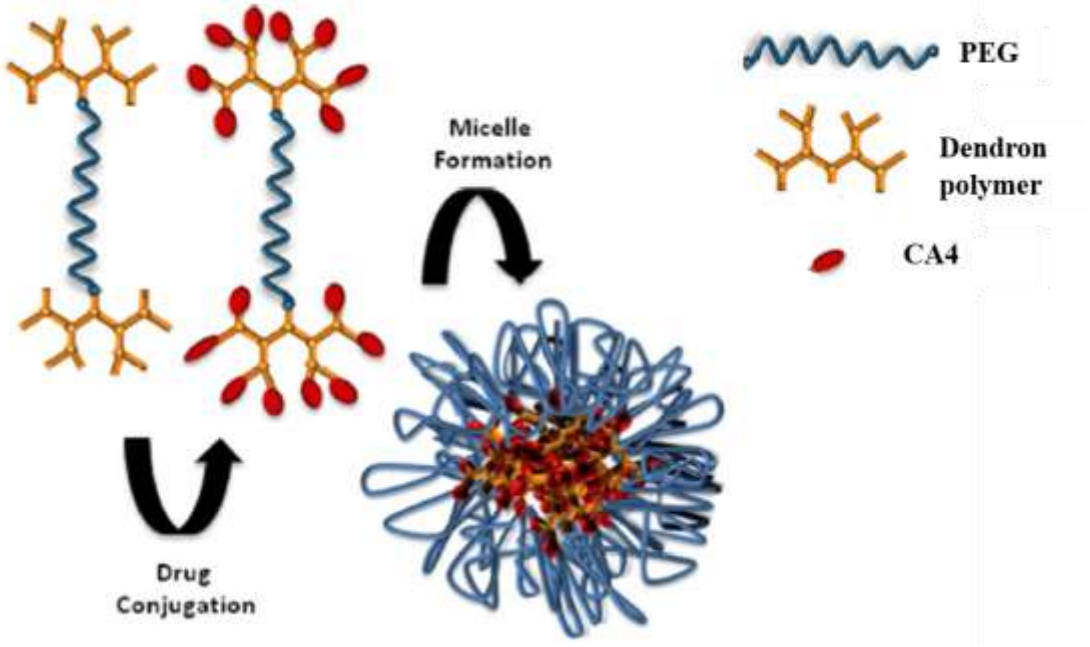

Figure 1.17: Schematic illustration of drug loaded micellar constructs from Dendron polymer conjugates (CA4-Dendron-PEG)[110].

In another study published in 2016, fabricated new CA4 nano-product was developed by Wu and co-workers using the covalent functionalization of graphene oxide with targeting peptide (NGR) to form GP-cNGR and non-covalently with CA4 (Figure1.18). *In vitro* studies showed a diminished cell viability in two tumor cell lines (HT-1080, MCF-7) [111].

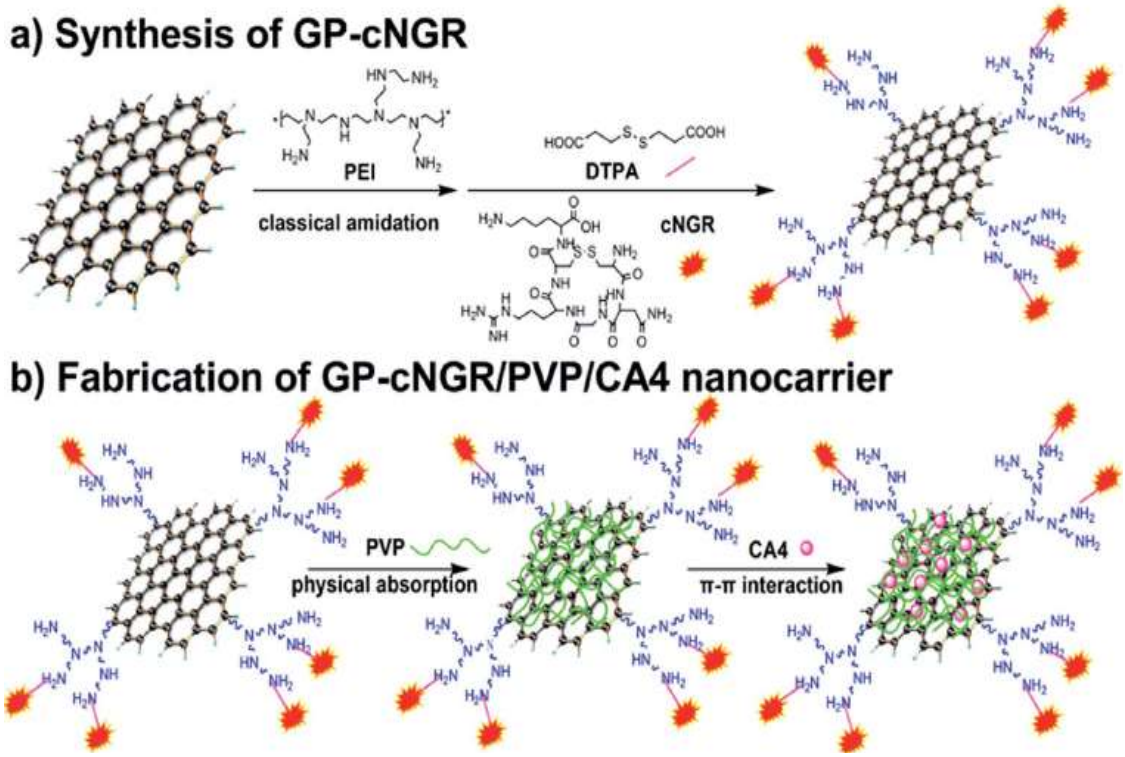

Figure1.18: (a) Covalent functionalization of NGR targeting peptide with graphene oxide. (b) Non-covalent functionalization of CA4 with the GP–cNGR/PVP nano-system[111].

To the best of our knowledge, although many studies have reported the conjugation of several nanomaterials with anti-cancer agents and their cytotoxicity against several cell lines, none of these studies have included the covalent functionalization of SWCNTs with CA4. In addition, no one of these studies have reported the antitumor activity and the dual functionalization of these anticancer agents with the targeting agent folic acid.

1.6. Aims of the study

The aim of our study is to develop a new nano-anticancer system based on covalent functionalization of SWCNTs with CA4 anticancer bound to PEG. Moreover, in order to develop a targeted nano anticancer system folic acid

was introduced through the dual functionalization of SWCNTs as shown in scheme 1. The anticancer activity was determined against HeLa cell line.

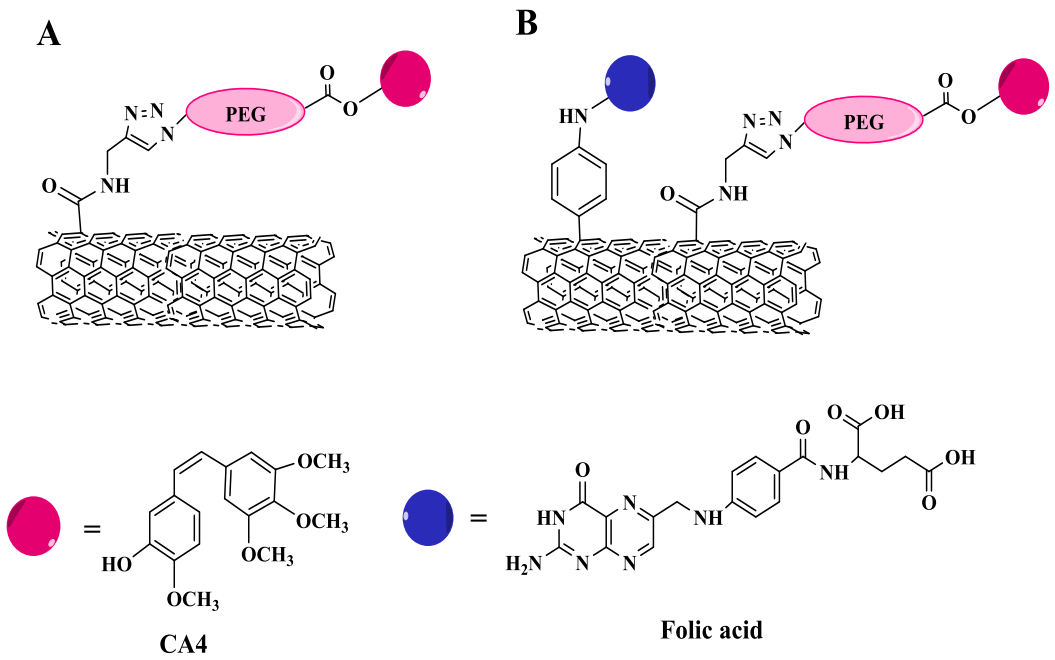

Scheme 1: (A) Covalent functionalization of SWCNTs with CA4. (B) Dual functionalization of SWCNTs with CA4 and folic acid.

1.7. Objectives

The objectives of the following research are:

1) Develop the high covalent functionalization of the SWCNTs in order to load the maximum possible quantity of the anticancer drug.

2) Improve total synthesis of CA4 and its attachment with the SWCNTs in order to improve its pharmacokinetic profile.

3) Dual functionalization of SWCNTs with both the targeting agent and the anticancer CA4.

4) Characterization of the formed nano anticancer drug by the different analytical techniques such as NMR, TEM, SEM, TGA and UV-Vis spectroscopes.

5) The determination of the anticancer activity by *in vitro* test and the comparison with the CA4 alone.

These objectives aim to develop a new and effective targeted nano-anticancer drug.

1.8. General approach of the synthesis and functionalization of SWCNTs

Scheme 2 summarizes the functionalization of SWCNTs and the covalent attachment of CA4 to the functionalized CNTs. This was obtained through multistage process that started with the synthesis of linker **(1)** from tetraethyelene glycol (TEG); the obtained linker was modified by NaN_3 to produce linker **(2)** which in turn was oxidized using John's reagent to produce linker **(3)**. An esterification reaction was used to attach linker **(3)** to CA4 in order to give the desired product **(5)**. In parallel to that; functionalized SWCNTs **(6)** was obtained by the reaction between propargylamine and carboxylated-SWCNTs through amidation reaction. The obtained alkyne-SWCNTs **(6)** was linked with compound (**5)** through Click reaction to get CA4-SWCNTs **(7)**.

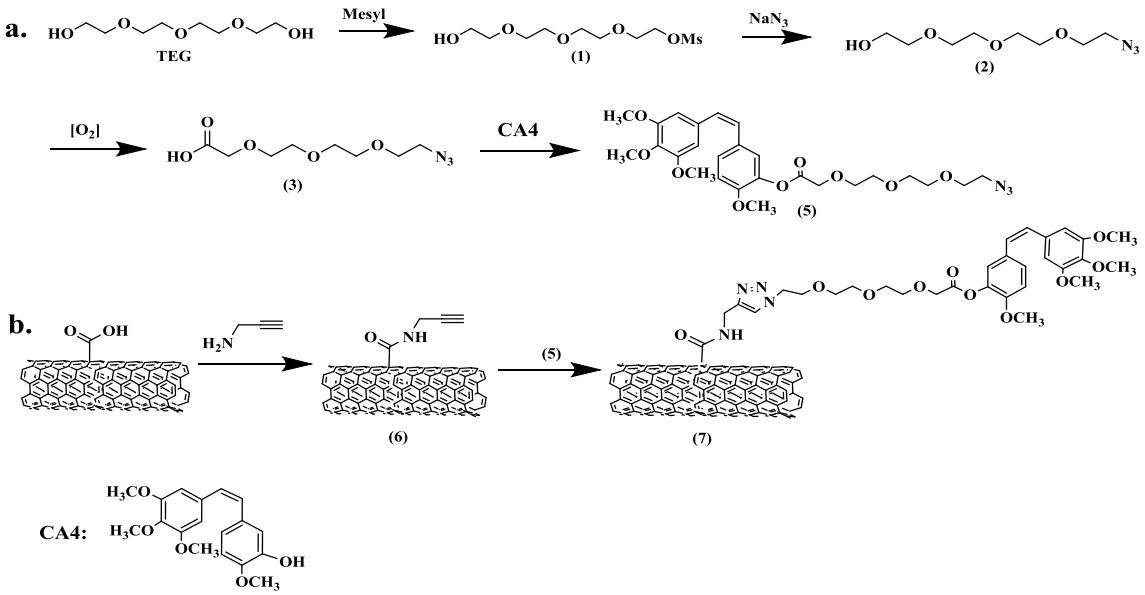

Scheme 2. Synthesis of: **a.**CA4-TEG-N_3 (**5)** and **b.** Functionalization of SWCNTs with **(5)**.

Scheme 3 summarizes the synthesis of product **13**, a dual-functionalized SWCNT. To achieve this, reagents **(8)** and **(9)** were initially prepared in order to functionalize the alkyne-SWCNT **(6)** with reagent **(9)** using Tour reaction to produce the *f*-SWCNT **(10).** After that**,** compound **(10)** was deprotected from Boc group to get *f*-SWCNTs **(11)**. Folic acid (FA), the targeting agent, was loaded firstly on the *f*-SWCNT **(11)** to synthesize the *f*-SWCNT **(12).** Then, the CA4-TEG-N_3 was linked to compound **(12)** *via* Click reaction to synthesis the final product CA4-FA-SWCNT **(13)**.

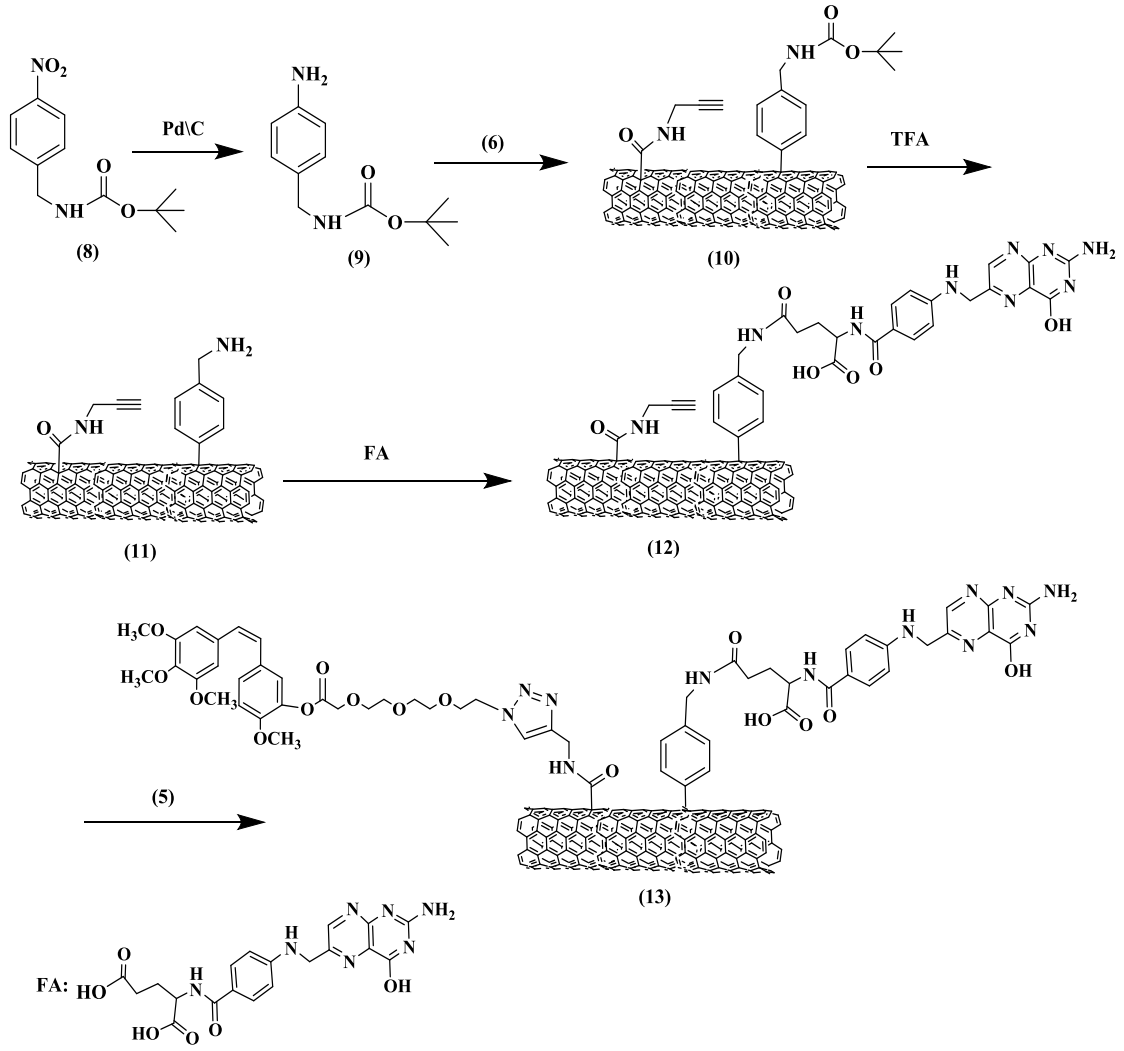

Scheme 3. Dual Functionalization of SWCNTs with CA4-TEG-N_3 **(5)** and folic acid.

Chapter Two
Materials and Methods

2.1. Materials

All materials that used in the experiments were of reagent grade. 2-(3,4,5-trimethoxyphenyl) acetic acid (catalog # B21136), 3-hydroxy-4-methoxybenzaldehyde (catalog # A12866), 1-(3-Dimethylaminopropyl)-3-ethylcarbodiimide hydrochloride (EDC) (catalog # A10807), L-ascorbic acid sodium salt (catalog # A17759), Porpargylamine (catalog # H53495), Trifluoroacetic acid (TFA) (catalog # A12198), and Tetraethylene glycol (catalog # B23990) were purchased from (Alfa Aesar Company, England). Quinoline (catalog # 43225) was purchased from (Alfa Aesar Company, India). SWCNT-COOH was brought from (carbon solutions, USA). Sodium azide (catalog # 0E30428), 1,2-Dichlorobenzene (*o*-DCB) (catalogue # 65152), 1,4-dioxane (catalog # 33147) solvents were purchased from (Riedel-de Haën Company, Germany). 4-[N-Boc)aminomethyl]aniline (catalog # 1001918209), Palladium on carbon (catalog # 101375286), 4-(dimethylamino) pyridine (DMAP) (catalog # 1122583), Isoamyl nitrite (catalog # 110463), 4-nitrobenzylamine hydrochloride(catalog # 191434), folic acid (catalog # F-7876), acetic anhydride (catalog # 320102), copper (catalog # 266086), Anhydrous copper sulfate (catalog # 451657), N,N-diisopropylethylamine (DIPEA) (catalog # 496219) and Di-tert-butyl dicarbonate (BOC_2O) (catalog # 101281549) were purchased from (Sigma-Aldrich, USA). Methanol (MeOH), dichloromethane (DCM), Isopropyl alcohol, Acetone

and ethanol were purchased from (C.S. Company, Israel). Ethyl acetate (EtOAc) (catalogue # 2355516100024), n-hexane (Hex) (catalogue # 2355544800024) and acetonitrile (CH_3CN)(catalogue # 5550070) solvents were purchased from (Frutarom Company, Isreal). Chloroform ($CHCl_3$) (catalogue # 67-66-3) was purchased from (merckmillipore) and tetrahydrofuran (THF) solvent (catalogue # 487308) was purchased from (Carlo Erba Company, MI. Italy).

All reactions were stirred under ambient conditions. Column chromatography using silica gel (pore size 60 Å, 40-63 µm particle size, 230-400 mesh particle size) purchased from Sigma Aldrich Company was used to purify the products. TLC (DC-Fertigfolien Alugeram®Silg/Uv_{254}, Macherey Nagel Company, Germany) was used to monitor the reactions. Centrifuge (UNIVERSAL 320, Hettich Zentrifugen, Germany) and water path sonicator (MRC DC-200H Digital Ultrasonic Cleaner) were used in preparation and dispersion of functionalized SWCNT. Rotary Evaporator (MRC, ROVA-100, laboratory equipment manufacturer) was used for solvents drying.

For biological test, Dulbecco's free Ca^{++} -phosphate buffered saline (REF # 02-023-1A), DMEM (REF # 01-055-1A), L-glutamine solution (REF # 03-020-1B) were purchased from (Biological industries, Israel). Trypsin-EDTA solution 1X (catalog # 59417C) and Calf-serum-iron fortified (catalog # C8065) were purchased from (SIGMA-ALDRICH, USA). Celltiter 96®Aqueous one solution cell proliferation Assay (# G3580,

USA). Annexin-V-FLUOS-staining Kit (# 11858777001) was purchased (Roche diagnostics, Germany).

2.2. Techniques and equipment

- **Nuclear Magnetic Resonance (NMR) spectra** were obtained using Bruker Avance 300 spectrometer, Switzerland).
- **Ultraviolet-Visible (UV-Vis) spectra** were recorded with (7315 Spectrophotometer, Jenway, UK), using quartz cuvettes.
- **Thermogravometric analysis spectra** were recorded by (STA 409 PC Luxx®, NETZSCH) in range 0-600 ºC, flow 20 ºC under nitrogen (100 cc/min).
- **Transmission Electron Microscopy (TEM)** images were taken by using Morgagni 286 transmission microscope (FEI Company, Eindhoven, Netherlands) at 60 kV.
- **Scanning Electron Microscopy (SEM)** images were taken by Inspect F50 SEM (FEI Company, Hillsboro, USA) with 1,000,000 times magnification.
- **Infrared spectroscopy (IR):** Nicolet iS5, ThermoFisher Scientific Company, USA.
- **Flow cytometry:** FACS caliber, Becton Dickinson, Immuno-fluorometry systems, Mountain View, CA.
- **High performance liquid chromatography (HPLC) dionex ultimate 3000.**

2.3. Synthesis and characterization of the products:

All the synthetic procedures and anticancer activity were prepared at An-Najah University laboratories. NMR measurements, SEM, TEM and TGA measurements, were conducted at the University of Jordan. HPLC was conducted at Dana Factory for Veterinary Medicines in Nablus.

2.3.1. Synthesis of 11-Mesyl-3,6,9-trioxaundecan-1-ol (1)

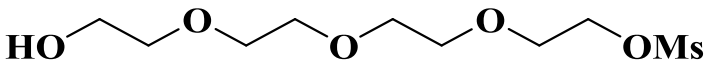

(1)

To a solution of tetraethylene glycol (10 g, 51.5 mmol) and triethylamine (7 ml, 51.5 mmol) in 50 ml THF stirred for 5 min and cooled at 0 ºC, mesyl chloride (4 ml, 51.5 mmol) was added dropwise over a period of 30min. The reaction was stirred vigorously for 24h at room temperature. The product was extracted with DCM (250 mL) and washed with HCl 1M (50 mL) and brine (50 mL). DCM was dried over Na_2SO_4, filtered and evaporated. The product was pale yellow oil purified by flash column chromatography in DCM/MeOH (20:1), TLC was visualized under UV light by DCM/MeOH (9:1) [112]. (Yield 28%, 4 g, 14.3mmol).

R_f: 0.5(DCM/MeOH 9:1).

^{1}H NMR (400 MHz, $CDCl_3$): δ 4.41-4.35 (m, 2H, $C\underline{H_2}OMs$), 3.81-3.60 (m, 14H, $7CH_2O$), 3.09 (s, 3H, $CH_2OSO_2C\underline{H_3}$), 2.97 (bs, 1H, OH).

^{13}C NMR (100.6 MHz, $CDCl_3$): δ 72.5 ($HOCH_2C\underline{H_2}O$), 70.4, 70.3, 70.1, 69.4, 69.3, 69.0 ($CH_2C\underline{H_2}OMs$), 61.6 ($OHC\underline{H_2}$), 37.6 (OSO_2CH_3).

2.3.2. Synthesis of 11-azido-3,6,9-trioxaundecan-1-ol (2)

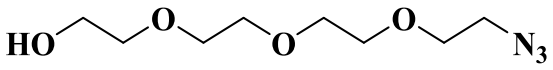

(2)

To a solution of compound **1**(1.8 g, 6.62 mmol) dissolved in 10 ml ethanol, sodium azide (515.97 mg, 7.94 mmol) was added. The reaction was stirred at 70 ºC overnight. Ethanol was evaporated and the reaction was extracted with 100 ml of diethyl ether and 40 ml of brine. Diethyl ether dried over (Na_2SO_4), filtered and evaporated the product was pale yellow oil [112]. TLC was visualized under UV light by DCM/MeOH (20:1). (Yield 85%, 1.23 g, 5.6 mmol).

R_f: 0.39 (DCM/MeOH 20:1).

^{1}H NMR (500 MHz, $CDCl_3$): δ 3.58 (t, 2H, *J*= 4.8 Hz, $HOC\underline{H_2}CH_2$), 3.55-3.51 (m, 10H, 5 CH_2O), 3.46 (t, 2H, *J* = 4.8 Hz, $OC\underline{H_2}CH_2N_3$), 3.26 (t, 2H, *J* = 4.8 Hz, $CH_2C\underline{H_2}N_3$), 3.10 (bs, 1H, OH).

^{13}C NMR (125.7 MHz, $CDCl_3$): δ 72.5 ($HOCH_2\underline{C}H_2O$), 70.6, 70.5, 70.4, 70.2, 69.9 (CH_2O), 61.5 (COH), 50.5 (CN_3).

IR: 3417.24, 2870.52, 2098.17, 1645.95cm^{-1}.

2.3.3. Synthesis of 11-azido-3,6,9-trioxaundecan-1-oic acid (3)

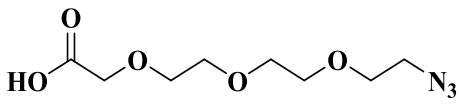

(3)

The Jones reagent (22 ml) was added to a solution of compound **2** (600 mg, 2.7 mmol) dissolved in acetone (22 ml), the reaction was stirred for 2h. After that, isopropyl alcohol was added to the reaction until became green. Then, the reaction solution was filtrated using Celite® and washed by DCM, the product was extracted by 40 ml of saturated $NaHCO_3$. The aqueous layer was washed with 100 ml of DCM and acidified with HCl (2M). DCM was dried over Na_2SO_4, filtrated and evaporated. The product was pale yellow oil [112]. (Yield 95%, 602 mg, 2.6 mmol).

R_f: 0.4(DCM/MeOH 9:1).

^{1}H NMR (500 MHz, $CDCl_3$):δ 9.30 (bs, 1H, COOH), 4.15 (s, 2H, $C\underline{H_2}COOH$), 3.80-3.60 (m, 10H, $5CH_2O$), 3.29 (t, 2H, J = 4.5 Hz, CH_2N_3).

^{13}C NMR (125.7 MHz, $CDCl_3$):δ 173.5 (CO), 70.9 ($\underline{C}H_2COOH$), 70.4, 70.3, 70.2, 69.9, 68.3 ($O\underline{C}H_2CH_2N_3$), 50.5 (CN_3).

IR: broad peak (2200-2600), 2921.63, 2853.17, 2108.78, 1714.41 cm^{-1}.

2.3.4. Synthesis of Combretastatin(CA-4) (4)

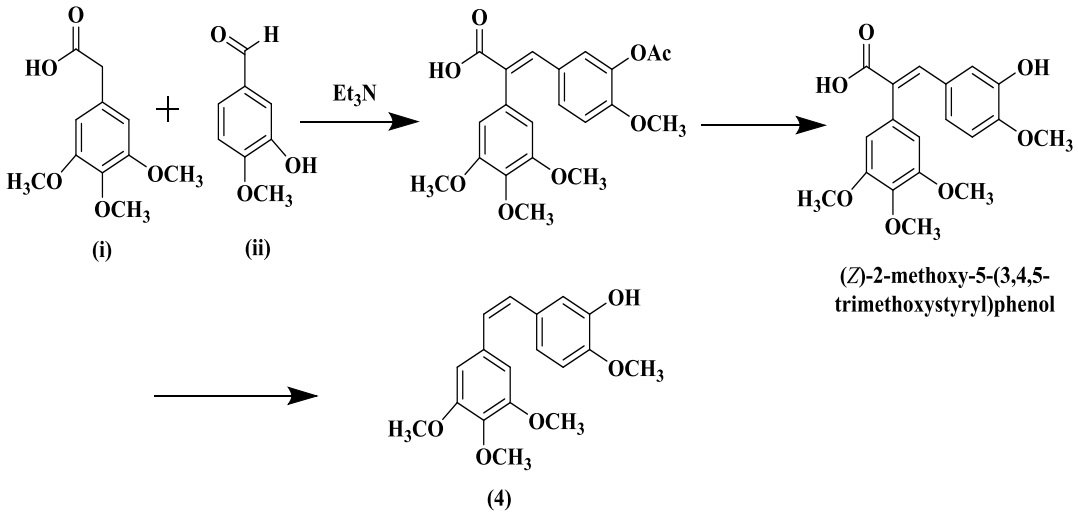

Scheme 4: Synthesis of CA4.

The CA4 was synthesized according to the method published by Xiao, et al. with some modification [113]. Triethylamine (2.22 ml, 15.91 mmol) was added to a solution of (2-(3,4,5-trimethoxyphenyl) acetic acid (i) (3 g, 13.26 mmol), 3-hydroxy-4-methoxybenzaldehyde (ii) (2.421 g, 15.91 mmol) and acetic anhydride (4.38 ml, 46.41 mmol). The reaction was kept at 110 ^{o}C for 4h. After that, the reaction was cold to room temperature (R.T) and acidified using HCl solution (2M). Then, the reaction was stirred in ice bath overnight. The obtained dark yellowish solid was dissolved in 10% NaOH (30 ml), washed and discolored with ethyl acetate (100 ml). HCl 2M was added until pH (3-4), the precipitated solid was filtrated and recrystallized from EtOAc to give the derivative of acrylic acid.

To derivative of acrylic acid (3.29 g, 9.16 mmol) and copper (4.66 g, 73.26 mmol) dried under vacuum and argon, quinoline (15 ml) was added. The

reaction was stirred at 200 ºC for 3h. After that, the reaction was cooled and filtrated. The filtrate was extracted with EtOAc (110 ml) and HCl 2M (60 ml), the EtOAc layer was washed with saturated NaCl (60 ml) and was dried over Na_2SO_4 to get brown viscous solid which purified by flash column chromatography in n-hexane/ethyl acetate (7:3). The recrystallized was achieved by ethyl acetate: petroleum ether to afford colorless crystals **(4)** (Yield 36.4%, 1.21 g, 3.8 mmol of product).

R_f: 0.23 (Hex/EtOAc7:3).

^{1}H NMR (300 MHz, $CDCl_3$):δ 6.90 (s, 1H, CH, C10 Ar), 6.77 (d, *J* = 8.19 Hz, 1H, CH, C11 Ar), 6.71 (d, *J* = 8.19 Hz, 1H, 1CH, C13 Ar), 6.51(s, 2H, 2CH, Ar), 6.39 (d, *J* = 12.1 Hz, 1H, CH=CH), 6.45 (d, *J* = 12.1 Hz,1H ,CH, CH=CH), 5.50 (s, 1H, OH), 3.82-3.84 (s, 6H, $2OCH_3$), 3.68 (s, 6H, $2OCH_3$).

IR: 3439.54, 2935.13, 2838.7, 1734.66, 1685.48, 1579.41, 1506.13 cm^{-1}.

HPLC: The purity of cis-CA4 was higher than 96% according to the HPLC measurements. A C-18 column (inertsil® OSD-3V, 4.6 x 250 mm, 5µm) was used with a mobile phase of 0.1%TFA in H_2O (eluent A) and 0.1%TFA in CH_3CN (eluent B). The eluent gradient was set from 20% to 100% B in 30min with a flow rate 1 ml/min and the pressure was 107 bar. The CA4 was detected by measuring absorbance at 295 nm.

2.3.5. Synthesis of CA4-TEG-N_3 (5)

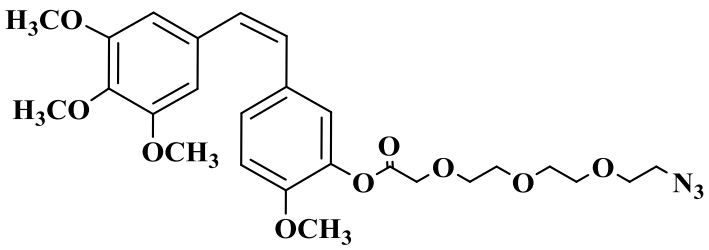

(5)

A solution of CA4 (200 mg, 0.629 mmol), compound **3** (221 mg, 0.95 mmol), EDC (182 mg, 0.95 mmol) and 4-(dimethylamino)pyridine (116 mg, 0.95 mmol) in dichloromethane (5 ml) was stirred for 19h under argon. The reaction was extracted with 40 ml of HCl (1M) and 120 ml DCM, aqueous layer was washed with DCM (2 x 50 ml), and the organic layer was dried over Na_2SO_4, filtrated and evaporated. The product was purified by silica gel by Hex/EtOAc (1:1). (Yield 69%, 233 mg, 0.44 mmol).

R_f: 0.23 (Hex/EtOAc1:1).

^{1}H NMR (300 MHz, $CDCl_3$):δ 7.06 (d, 2H, 2CH, Ar), 6.95 (d, 1H, CH, Ar), 6.78 (d,*J*= 8.56 Hz, 2H, 2CH, Ar), 6.39 (d, *J*= 12.1 Hz, 1H, CH=CH), 6.45 (d, *J* = 12.1 Hz, 1H, CH, CH=CH), 4.33 (s, 2H, CH_2, $COOCH_2$),3.95-3.76 (m, 22H, CH_2/CH_3, OCH_2CH_2O/OCH_3), 3.3 (t, 2H, *J* = 5.87 Hz CH_2, CH_2N_3).

^{13}C NMR (125.7 MHz, $CDCl_3$):δ 50.70, 55.95, 60.90, 68.33, 70.05, 70.66, 70.68, 70.96, 105.90, 112.08, 123.02, 127.90, 128.47, 129.71, 130.20, 132.39, 137.24, 138.96, 150.07, 153.01, 168.46.

IR: 2961.16, 2922.59, 2102.03, 1776.12, 1613.16, 1578.45, 1507.1 cm^{-1}.

2.3.6. Functionalization of carboxylated-SWCNTs with proprgy lamine (6).

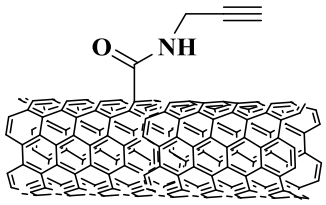

(6)

To carboxylated SWCNTs (75 mg) solubilized in DMF (30 ml). EDC (30 mg, 0.16 mmol) and triethylamine (300 µl, 2.19mmol) were added. The solution was sonicated for 1h, then the propargylamine (52 µl, 0.82 mmol) was added. The reaction was sonicated for 10min and stirred for 72h. $CHCl_3$ (25 ml) was added to reaction, centrifuged for 10min at 15,000 rpm, supernatant was discarded. Washing process was repeated with $CHCl_3$ (2 x 20 ml), DCM (10 ml) and diethyl ether (2 x 10 ml). The black powder was dried under vacuum. The obtained weight was 69 mg.

2.3.7. Functionalization of Alkyne-SWCNTs with compound 5 (7)

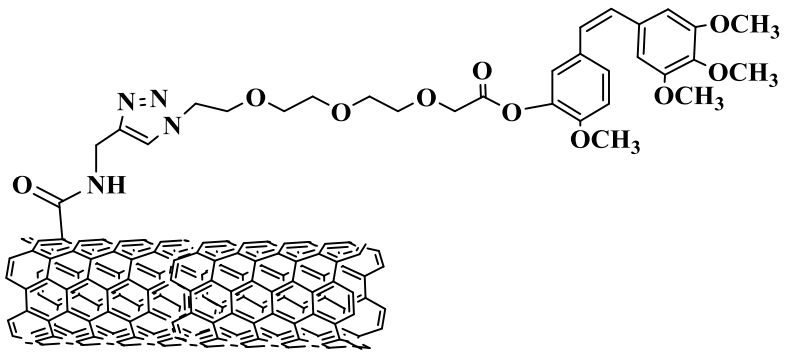

(7)

To anhydrous copper sulfate (anhydrous $CuSO_4$) (7.9 mg, 0.05 mmol), L-ascorbic acid sodium salt (3 mg, 0.02 mmol) dissolved in 4 ml of distilled H_2O was added, the solution was added to a sonicated solution of CA4-

TEG-N_3**5** (65 mg, 0.11 mmol), and Alkyne-SWCNTs **6** (30 mg) dissolved in 4 ml of DCM. The solution was sonicated for 10min. The reaction was stirred overnight. MeOH (15 ml) was added to reaction, sonicated then centrifuged at 15,000 rpm for 10min, supernatant was discarded followed by two washing steps with MeOH (2 x 15 ml) and ether (2 x 15 ml), black powder was dried. The obtained weight was 25 mg.

2.3.8. Synthesis of 4-nitro benzylamine-BOC (8)

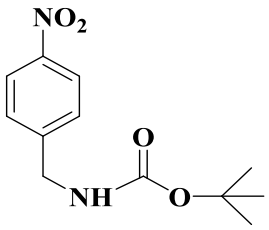

(8)

To a solution of 4-nitro benzyl amine (408 mg, 2.159 mmol) dissolved in 8 ml water/Dioxane (4:4) and NaOH 1M (18 ml), BOC_2O (519.3 mg, 2.38 mmol) was added. The reaction was stirred at R.T overnight. The reaction was filtered by suction filtration and dried. The final product was purified by column chromatography in n-hexane/ethyl acetate (2:1). (Yield 67%, 366 mg, 1.45 mmol, white powder).

R_f: 0.35 (Hex/EtOAc2:1).

^{1}H NMR (300 MHz, $CDCl_3$):δ 7.20 (d, *J* = 8.2 Hz, 2H, 2CH, Ar), 6.76 (d, *J* = 8.6 Hz, 2H, 2CH, Ar), 4.88 (bs, 1H, NH), 3.71 (bs, 2H, $C\underline{H_2}Ar$), 1.48 (s, 9H, $3CH_3$, boc).

^{13}C NMR (300 MHz, $CDCl_3$):δ 155.64, 145.06, 128.50, 128.09, 121.83, 84.75, 45.10, 27.52.

2.3.9. Synthesis of 4-(Boc-amino)benzylamine (9)

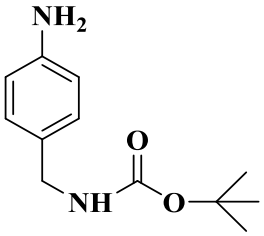

(9)

To a solution of compound **8** (245 mg, 0.97 mmol) dissolved in 10 ml acidic ethanol (by adding 30 drops of 1.0 M HCl), 11 mg of palladium on carbon (10%) was added. The reaction mixture was stirred under H_2 at R.T overnight. Ethanol was evaporated, the reaction was filtrated and purified by flash column chromatography in Hex/EtOAc (2:1). (Yield 91%, 197 mg, 0.88 mmol).

R_f: 0.167 (Hex/EtOAc2:1).

^{1}H NMR (300 MHz, $CDCl_3$):δ 7.10 (d, *J* = 8.1 Hz, 2H, 2CH, Ar), 6.66 (d, *J* = 8.4 Hz, 2H, 2CH, Ar), 4.70 (bs, 1H, NH), 4.11 (d, *J* = 5.4 Hz, 2H, NH_2) 3.71 (bs, 2H, $C\underline{H_2}Ar$), 1.46 (s, 9H, $3CH_3$, boc).

^{13}C NMR (300 MHz, $CDCl_3$):δ 156.64, 145.86, 128.00, 127.91, 115.83, 80.75, 43.12, 28.72.

2.3.10. Functionalization of Alkyne-SWCNTs with compound 9 (10)

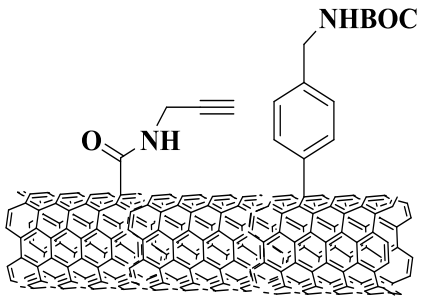

(10)

To compound **9** (107 mg, 0.45 mmol) and alkyne-SWCNTs **6** (30 mg) dried under vacuum and argon, 1,2-dichlorobenzene (13 ml) and acetonitrile (8 ml) were added. The reaction was sonicated for 10min. After bubbling with argon, 362 µl of isoamyl nitrite was added dropwise to the reaction, then stirred and heated at 60 ºC for 24h under argon [73]. Functionalized SWCNTs were washed with 20 ml of MeOH, and centrifuged at 15,000 rpm for 10min washing steps were repeated with MeOH (2 x 15 ml), with DCM (15 ml) and ether (2 x 15 ml). The product was dried. The weight of dried black powder was 34 mg.

2.3.11. Deprotection of BOC group in compound 10 (11)

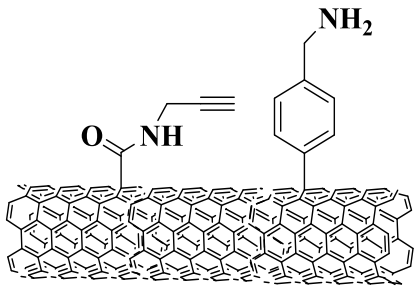

(11)

To *f*-SWCNTs **10** (28 mg) solubilized in 3.4 ml of DCM and sonicated for 10min, TFA (2.3 ml) was added, reaction and stirred overnight. 20 ml of MeOH was added then sonicated and centrifuged at 15,000 rpm for 10min. Washing steps were repeated with MeOH (2 x 15 ml), DCM (15 ml) and ether (2 x 15 ml). The obtained Weight of the dried black powder was 25 mg.

2.3.12. Quantitative KaiserTest protocol [to determine the free NH_2 loading].

The experiment was done in according to the literature and the result was expressed as μmole of amino groups per gram of SWCNTs [114, 115].

2.3.13. Functionalization of *f*-SWCNTs 11 with folic acid (12)

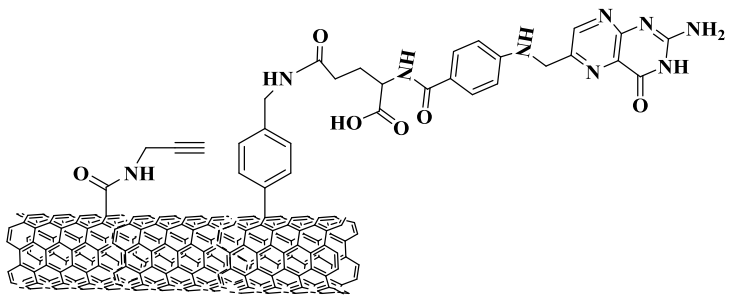

(12)

4 ml of dimethylformamide was added to RBF contain folic acid (44 mg, 0.1 mmol), EDC (38.34 mg, 0.2 mmol) and 4-(dimethylamino)pyridine (12.17 mg, 0.1 mmol) dried under vacuum and argon. The reaction mixture was stirred for 2h. In another RBF, dimethylformamide (4ml) was added to the 23.3 mg of *f*-SWCNTs (**11)** dried under argon, solution was sonicated for 10min. After 2h, the solution of folic acid reaction was added to *f*-SWCNTs (**11)** solution. The reaction was stirred for 24h under argon. 15 ml of MeOH was added to reaction and centrifuged at 15,000 rpm for 10min, supernatant was discarded. Washing steps were repeated with MeOH (2 x 10 ml), and ether (2 x 10 ml). Black powder was dried. The weight of obtained product was 32.6 mg.

2.3.14. Functionalization of *f*-SWCNTs 12 with compound 5 (13)

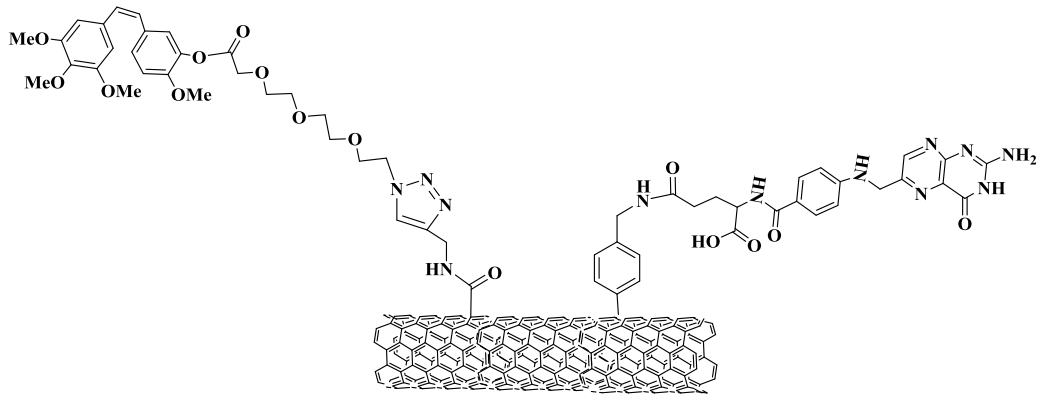

(13)

To anhydrous $CuSO_4$ (12 mg, 0.07 mmol), L-ascorbic acid sodium salt (5 mg, 0.02 mmol) dissolved in 3 ml of distilled H_2O was added. The solution was added to a sonicated solution of CA4-TEG-N_3 **5** (97 mg, 0.16 mmol) and *f*-SWCNTs **12** (30 mg) dissolved in 3ml of DCM. The reaction was stirred for 24h. 15 ml of MeOH was added to reaction, sonicated and centrifuged at 15,000 rpm for 10min, supernatant was discarded, product was washed with MeOH (2 x 10 ml), and ether (2 x 10 ml). Black powder was dried. The obtained weight of the black powder was 22 mg.

2.4. In vitro drug release

In vitro release study, using dialysis bag diffusion technique in 10% fetal bovine serum (FBS) phosphate buffer saline, was conducted on compound **(7)** in order to estimate the kinetic release pattern of the CA4 from SWCNTs.

2.4.1. Preparation of Phosphate buffered saline (PBS)

1.0 L PBS (pH 7.4) was prepared according to the literatures [116, 117].

2.4.2. Calibration curve of Combretastatin A4

A calibration curve was developed by plotting absorbance *vs*. concentration in order to quantify the amount of loaded CA4 on SWCNTs.

Accordingly, CA4 stock solution was prepared by dissolving an accurately weighed (1 mg) of this compound in 10% FBS diluted with adequate volume of PBS. A series of dilutions (0.5, 0.3, 0.1, and 0.02 mg/ml) were prepared by diluting the required volume of the standard solution in adequate volume of solvent. The drug showed maximum absorbance at 300 nm (λ_{max}) and therefore it was selected for the assessment of its concentration.

2.4.3. Dialysis membrane method

An accurately weighed amount of compound **7** (1 mg) was dispersed in 1 ml of a freshly prepared 10% FBS phosphate buffer solution and transferred into the dialysis bag (spectra/Por® 4). The filled bag was immersed in 150 ml of the prepare PBS and kept under gentle and continuous stirring for 54hrs at 37 ºC. An aliquot was withdrawn from the release medium at each specified time periods and was replace with equal volume of fresh medium to mimic the sink condition. The absorbance of the collected samples was measured at 300 nm using UV/vis

spectrophotometer. The concentration of the released drug was calculated according to equation (y = 1.988x).

2.5. Anticancer activity

2.5.1. Cell line

The anticancer activity of compound (**7)** was studied against HeLa cells and compared to the activity of the free CA4.

2.5.2. Cell culture

HeLa cells were cultured in 15-cm^2 plastic culture plate in culture growth medium (CGM) which consists of DMEM medium supplemented with 10% fetal bovine serum (FBS), L-glutamine and penicillin/streptomycin. Cells were maintained in the above medium at 37°C in a humidified atmosphere containing 5% CO_2.

For sub-culturing, the CGM was suctioned from 15-cm^2 culture plate. Then, the cells were washed with 15 ml of Ca^{2+}-free PBS. After that, 5 ml of trypsin was added to cells and were incubated for 3 minutes in a humidified atmosphere containing 5% CO_2 at 37°C until sufficient cells detachment from the surface of the plates. After that, trypsin was inactivated by 20 ml of CGM, and subsequently the cell suspension was collected, diluted and distributed into 96-well plate or 12-well plate (according to the test) and were left to adhere over 24 hrs.

2.5.3. Cell viability test

The HeLa cells were subcultured into 96 well plate as explained above. After 24hrs, the cells were incubated with 100 µl of different concentrations of compound (**7)** for different time periods. After that, 20 µl of MTS solutions was added to each well followed by an incubation period of 1h before the absorbance was measured by a plate reader.

2.5.4. Flow cytometry analysis

The cells were subcultured into 12 well plate as explained above. After that, they were treated with different concentrations (5, 10 or 15 ng\ml) of CA4 and compound (**7)**; the cells were incubated with treatment solutions for 48hrs. After that, studies on apoptosis/necrosis and cell-cycle were conducted and were analyzed by Flow cytometry (FACS caliber, Becton Dickinson, Immuno-fluorometry systems, Mountain View, CA).

2.5.4.1. Apoptosis and necrosis assay

After 48hrs of incubation, both adherent and non-adherent cells were harvested manually in CGM, centrifuged for 10 min at RCF = 150 g and the supernatant was discarded. Then, 1.5 ml of PBS was added to the cell pellet, the cell suspension was centrifuged for 10 min at RCF= 150 g, and the supernatant was discarded. Then, 250 µl of Ca^{+2} free PBS was added to the cell pellet. The cells were treated with (5 µl\100 µl) of Annexin-V and incubated at room temperature (R.T) for 15 min. After that, cells were washed with PBS, centrifuged and incubated with (5 µl\500 µl) of

propidium iodide solution (PI) solution and the obtained stained cell suspension was analyzed by flow cytometery technique.

2.5.4.2. Cell cycle assay

After 48 hrs of incubation with the treatment conditions, the adhered and non-adhered cells were harvested and centrifuged at RCF= 150 g for 10 min. The supernatant was discarded. 1 µl of 70% MeOH was added to the cell pellet and incubated at -20 ºC for 20 min to permeabilize the cell membrane. The pellet was then washed with 1.5 ml of PBS and centrifuged at RCF= 150 g for 10 min. Then, the supernatant was discarded and the pellets were resuspended in propidium iodide solution (PI) and was incubated for 15min before being analyzed with FACS. Data analysis was carried out using FCS express 6 (De novo software).

Chapter Three
Results and Discussion

3.1. Synthesis and functionalization of SWCNTs

In order to functionalize SWCNTs with CA4, the TEG was used as linker between CA4 and SWCNTs. The linker was synthesized using several steps started with the reaction of OH group of TEG with mesyl group to get compound **(1)**. After that, the mesyl group was replaced with N_3 through the reaction of **(1)** with NaN_3 in ethanol to get TEG-N_3 **(2)**. Compound **(2)** oxidized by Jone's reagent to prepare linker **(3)** followed by esterification reaction of linker **(3)** with compound **(4)** through using EDC as a coupling agent and DMAP as a catalyst to synthesized compound **(5)** as shown in Scheme 5.

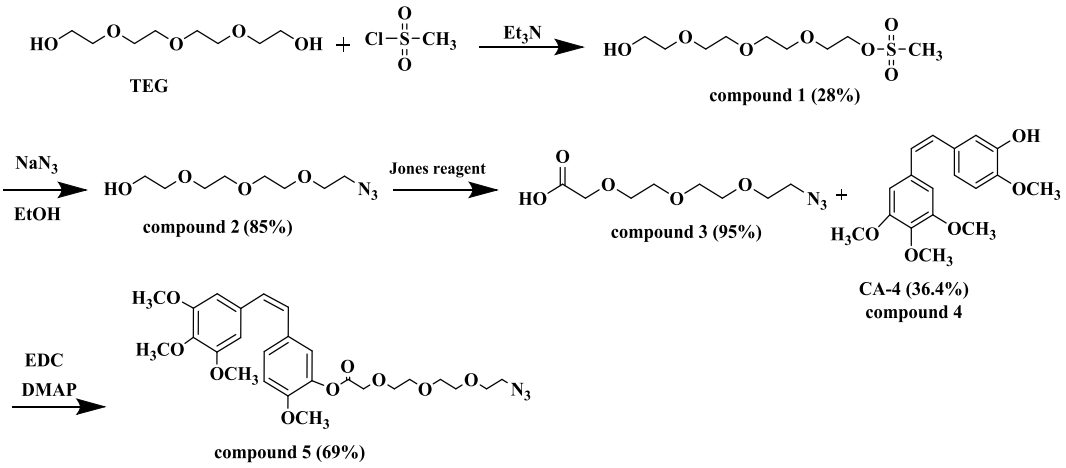

Scheme 5. Synthesis of CA4-TEG-N_3 (**5**).

The basic chemical structure of the compound (**5**) was confirmed by NMR. The CH of aromatic ring was appeared in range (6.78-7.06) ppm. The *cis* CH=CH was appeared between (6.39-6.45) ppm. The CH_2 of CH_2COO was

appeared in 4.33ppm. The CH_2 of TEG and CH_3 of OCH_3 were appeared between (3.95-3.76) ppm and the CH_2 of CH_2-N_3 was appeared in 3.3 ppm.

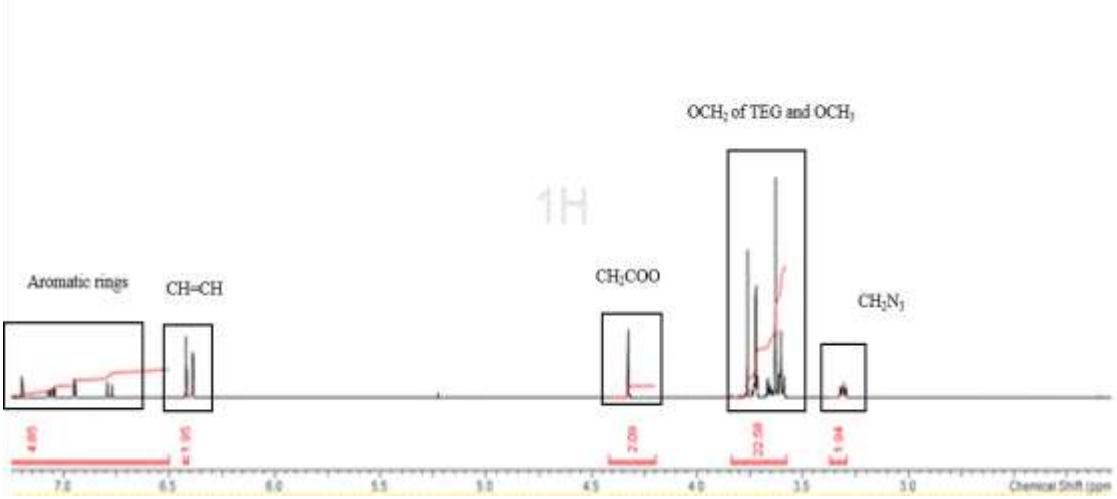

Figure 3.1: H^1 NMR spectrum of CA4-TEG-N_3 (**5).**

After the successful synthesis of CA4-TEG-N_3, the carboxylated-SWCNTs were functionalized covalently with propargylamine through amidation reaction to get terminal alkyne group. After that, the alkyne-SWCNTs **(6)** were effectively bind with compound **(5)** through click reaction by using anhydride.$CuSO_4$ and ascorbic acid as catalysts which dissolved in DCM and water to synthesized CA4-CNTs **(compound 7)** as shown in the Scheme 6.

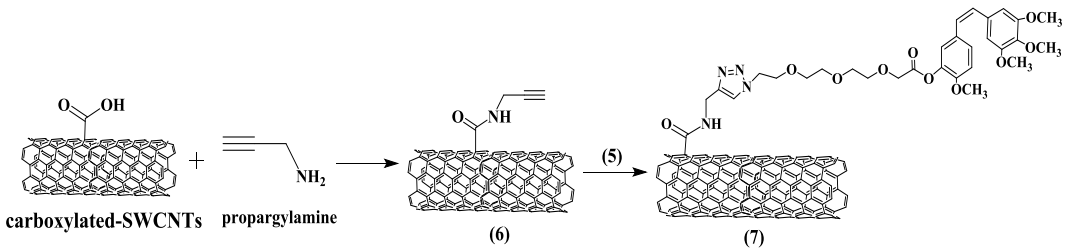

Scheme 6: Functionalization of alkyne-SWCNTs (**6)** with compound (**5).**

The dual functionalization of SWCNTs was achieved in order to selectively deliver CA4 by using folic acid as targeting agent since this agent is highly demanded by the cancer cells due to the over-expression of folic acid receptors [118]. The alkyne-SWCNTs **(6)** were covalently functionalized using the diazonium salt arylation reaction. The arylation of CNTs with diazonium salts was developed by the group of Tour [71]. The 4-(Boc amino) benzylamine was introduced on the functionalized SWCNTs. The resulting derivative was deprotected in acidic medium as shown in scheme 7. The corresponding amine loading value was determined by Kaiser test [119]. The total amine loading was 0.69 mmol per gram of SWCNTs. After that, the introduction of folic acid on the surface of SWCNTs (**11)** was conducted by forming amide linkage using EDC as coupling agent and DMAP as catalyst in order to obtain *f*-SWCNTs (**12)**. Then, the click reaction was performed between CA4-TEG-N_3 **(5)** and *f*-SWCNTs (**12)** to get CA-FA-SWCNTs (**13)** as shown in the Scheme 7.

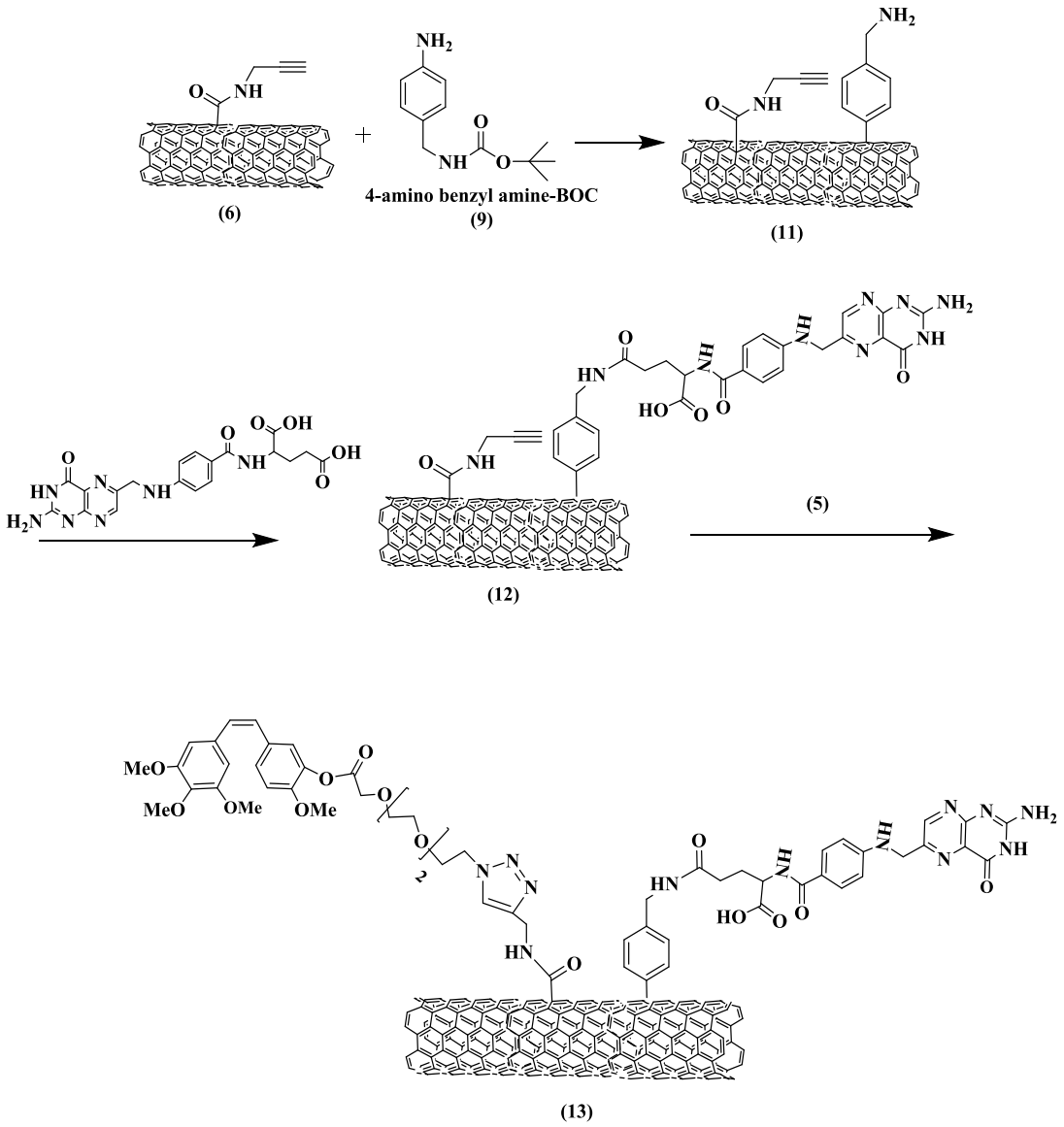

Scheme 7: Functionalization of alkyne-SWCNTs (**11)** with folic acid and compound (**5).**

3.2. Characterization of CA4-SWCNTs and CA4-FA-SWCNTs

3.2.1. Dispersibility of CNTs

After the functionalization of SWCNTs, the dispersibility of *p*-SWCNTs, CA4-SWCNTs (**7)** and CA4-FA-SWCNTs (**13)** in water was conducted. The *p*-SWCNTs (a) formed a clear black sediment after being suspended in water, while compound **7** (b) and **13** (c) showed a good water dispersibility (Figure 3.2). In fact, the *p*-SWCNTs have hydrophobic characteristics which encourage the rapid reaggregation of these nanotubes. On the other hand, the stable black suspensions of compounds (**7)** and (**13)** were due to the increase in the hydrophilicity which was gained by the new functionalization of SWCNTs.

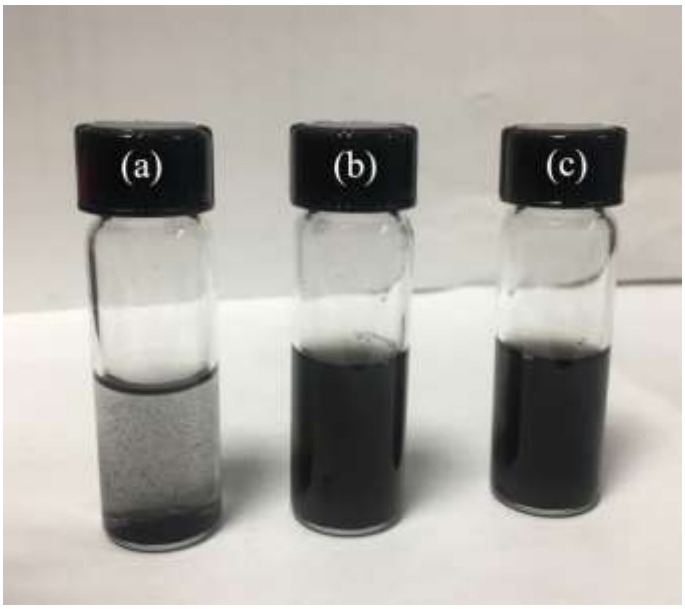

Figure 3.2: Photograph of dispersions of (a) *p*-SWCNTs, and (b) CA4-SWCNTs (**7)** and (c) CA4-FA-SWCNTs (**13).**

3.2.2. Morphology and size of SWCNTs

The morphology and the size of compounds (**7)** and (**13)** were investigated by TEM and SEM images (Figure 3.3 and 3.4). In these images the *p*-SWCNTs appeared as aggregated nanotubes. On the other hand, the functionalized compounds (**7)** and (**13)** appeared as individual separated nanotubes with diameter in the range of (5-15) nm. In fact, the chemical functionalization of the SWCNTs caused a separation and de-bundling effect due to the decrease in the hydrophobic interaction between the nanotubes side walls.

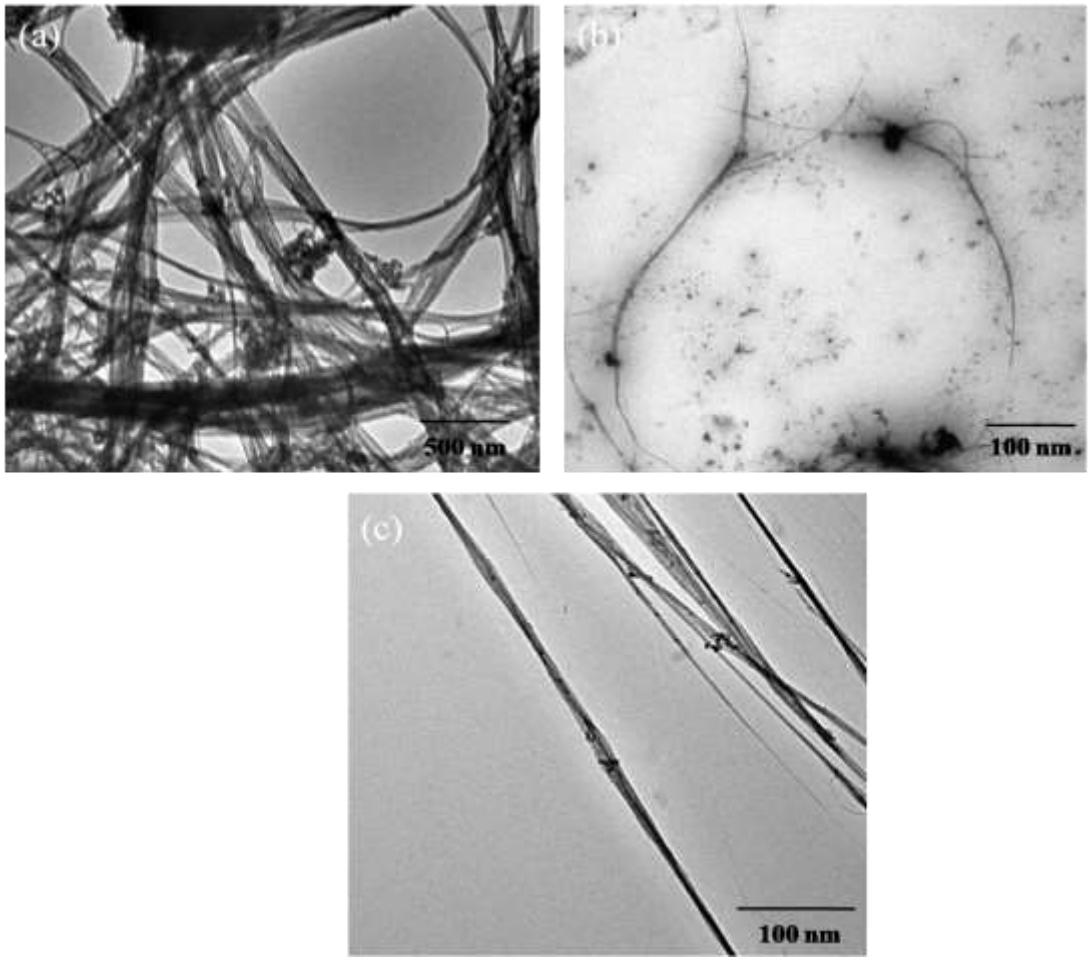

Figure 3.3: .TEM images: (a) *p*- SWCNTs, (b) CA4-SWCNTs (**7)**, (c) CA4-FA-SWCNTs (**13).**

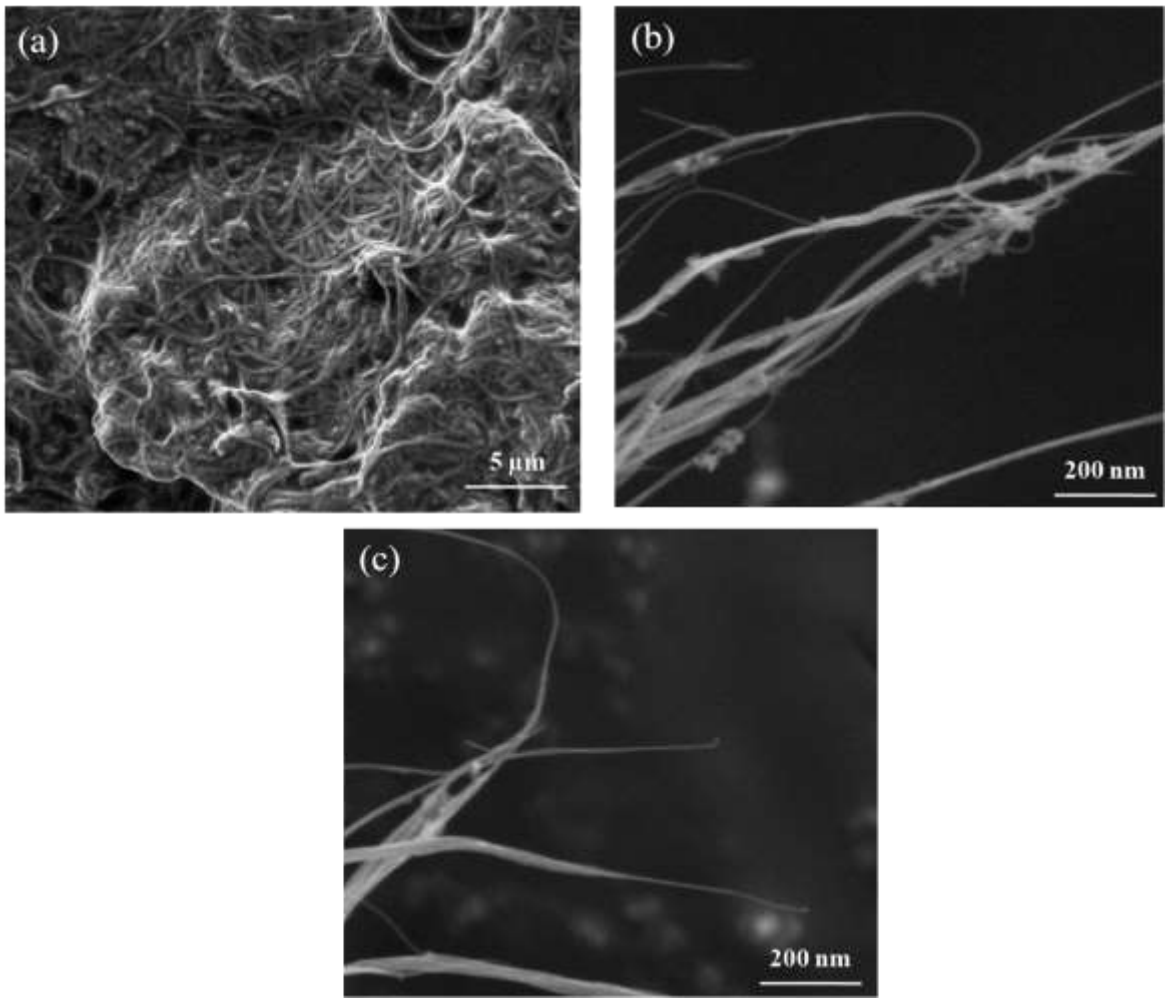

Figure 3.4: SEM images:(a) *p*-SWCNTs, (b) CA4-SWCNTs **(7)**, (c) CA4-FA-SWCNTs **(13).**

3.2.3. UV-vis spectrophotometery

The loaded amount of CA4 was measured by spectrophotometery. A calibration curve of CA4 has been built. The maximum absorption was observed at 300 nm and R^2 was higher than 0.99 (Figure 3.5). The loaded amount of CA4 on SWCNTs was about 0.223 mg in 1 mg of CA4-SWCNTs **(7)**.

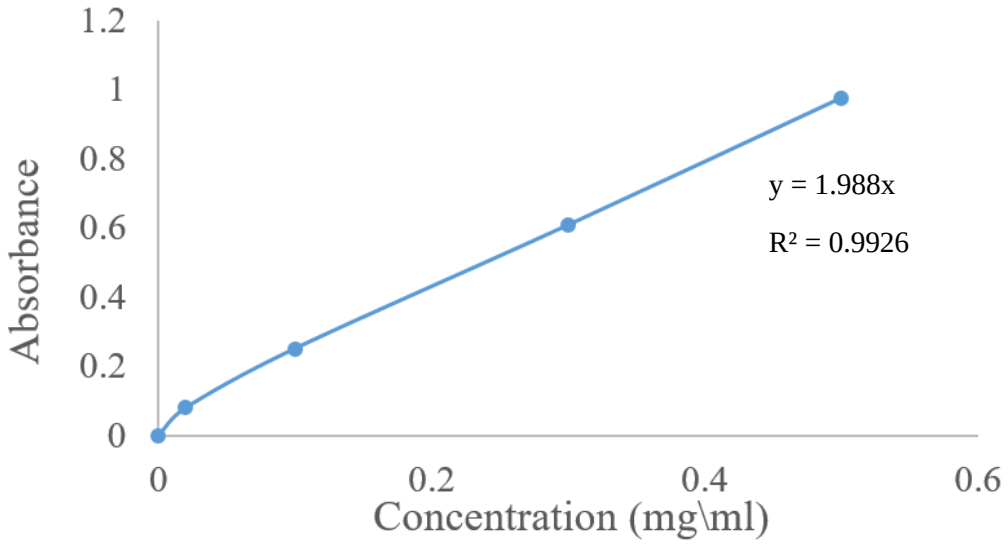

Figure 3.5: Calibration curve of CA4.

3.2.4 Thermogravometric analysis (TGA)

The mass loss was approximately 45% at 1000 °C (Figure 3.6). According to the MW of both CA4 and compound (**5**), the exact percent of loaded CA4 was about 23% w/w.

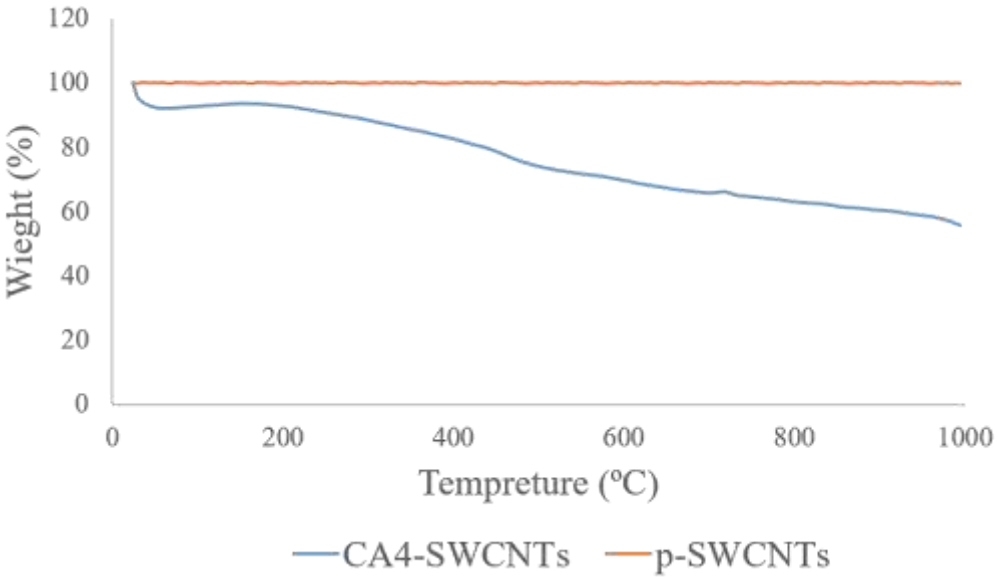

Figure 3.6: The TGA of CA4-SWCNTs.

Moreover, the percentage of functionalization of CA4-FA-SWCNTs (**13)** was also determined by TGA. At 1000 °C, compound **(13)** showed a mass loss of 50.4% as shown in Figure 3.7. More precisely, the percentage of loaded CA4 and FA on compound (**13)** was 14% w/w and 19%w/w respectively.

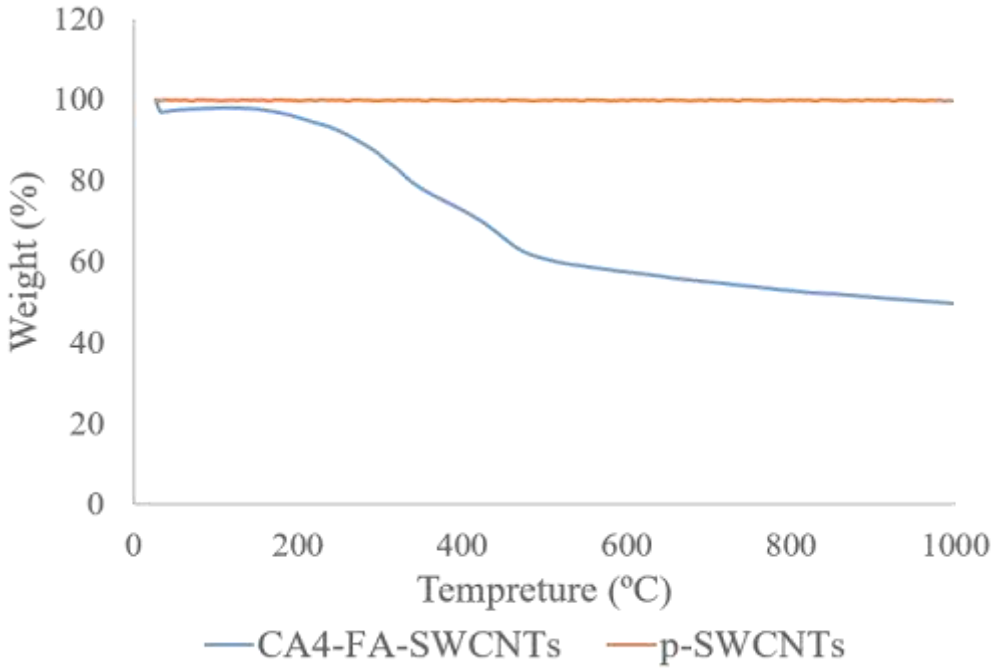

Figure 3.7: The TGA of CA4-FA-SWCNTs **(13)**.

3.3 *In vitro* drug release

A time dependent cumulative release of CA4 from compound (**7)** was conducted in 10% FBS in phosphate buffer at pH 7.4 and kept at 37 ºC. About 90% of the loaded CA4 was released in 50 hrs. 32% release after 6 hrs while approximately 74% of loaded CA4 was release after 24 hrs as shown in Figure 3.8.

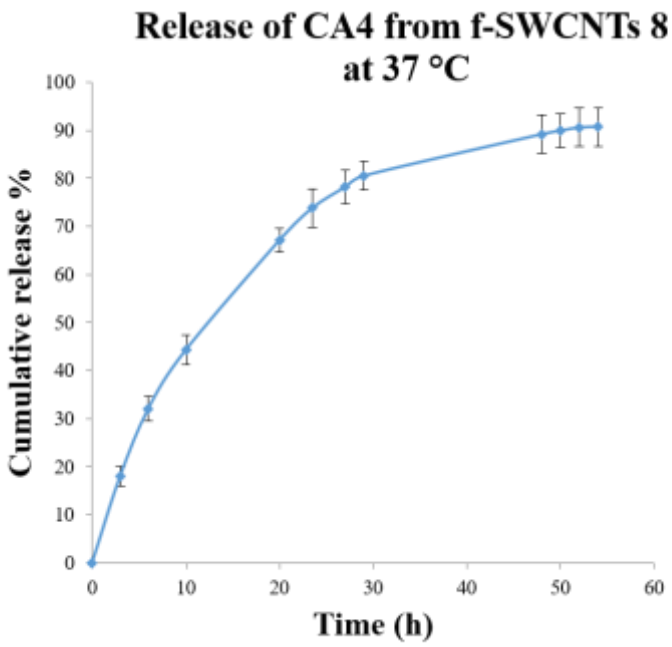

Figure 3.8: *In vitro* release of CA4 from compound **(7)** up to 50 h in phosphate buffer (10% FBS) solution kept at pH 7.4 at 37 ºC

3.4. Anticancer activity

HeLa cells were used to investigate the therapeutic efficacy of functionalized compound **(7)**. Free CA4 and cell without treatments where used as controls. The therapeutic efficacy was qualitatively confirmed by microscopic visualization of the morphology of treated cells for 48 hrs. The treatments with free CA4 and compound **(7)** induced significant changes in cell morphology, as the majority of the cells became rounded and detached (Figure 3.9). The *MTS Proliferation assay* (MTS) was used to evaluate the therapeutic efficacy of functionalized CNTs and to select the appropriate concentration of the treatment by treating cells with different concentrations (15, 30 and 60 ng/ml).

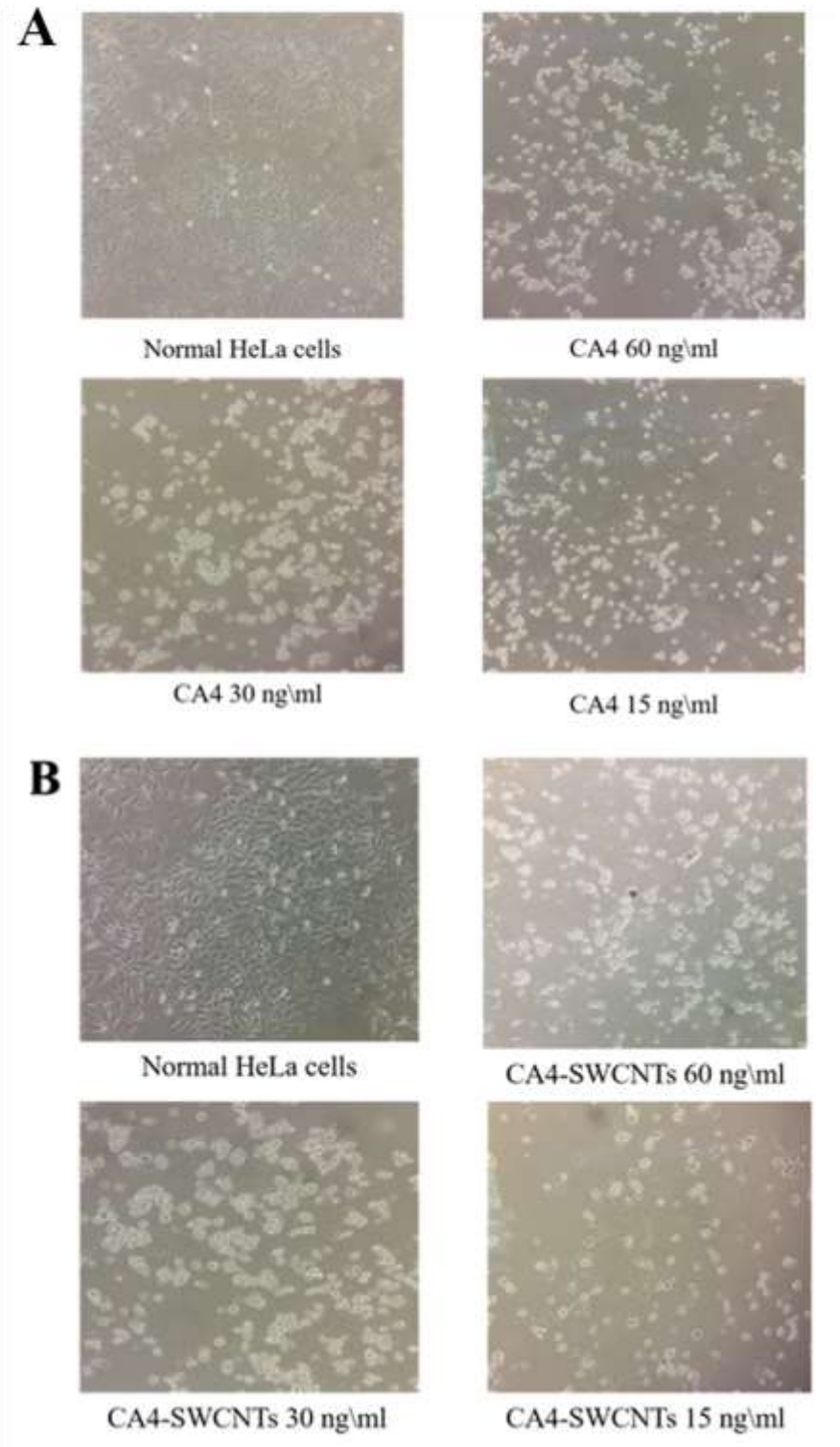

Figure 3.9: The morphology changes of HeLa cells upon treatment with different concentrations of: (A) CA4 (15, 30 and 60) ng\ml. (B) CA4-SWCNTs (**7)** (15, 30 and 60) ng\ml.

The results showed that the concentrations 30 and 60 ng/ml were too much cytotoxic, therefore a lower concentration (15 ng/ml) was selected since it showed cytotoxic effect but still enough cells were still adhered. Also, the MTS assay was done to determine the time needed by our compound (15 ng/ ml) to cause an adequate effect. From the time response relationship shown in Figure 3.10, a 48 hrs was found as the appropriate time.

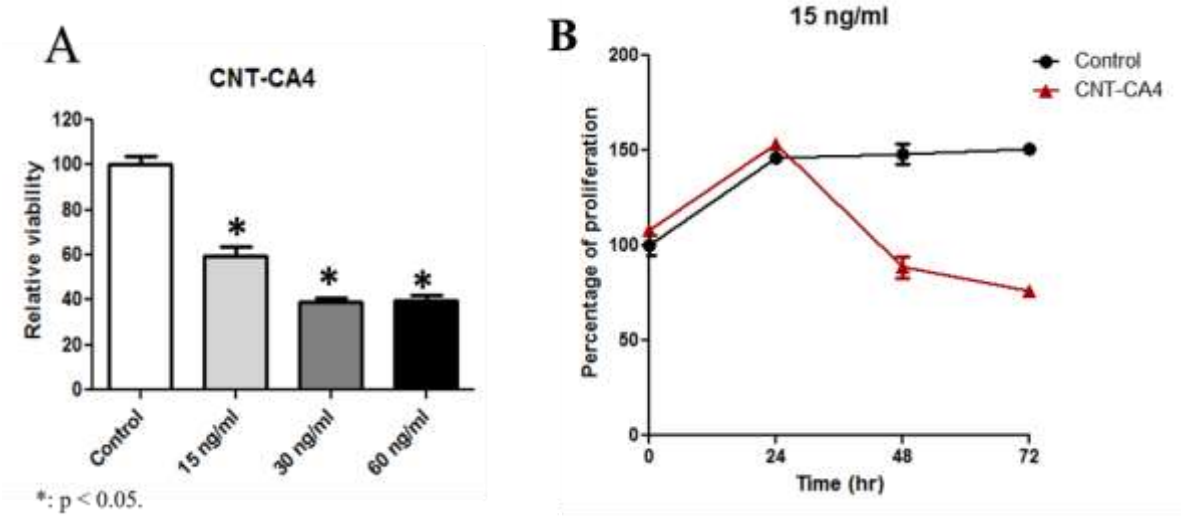

Figure3.10: A. The therapeutic efficacy of compound **(7)** at different concentrations (15, 30 and 60) ng\ml. B. The time response relationship of compound **(7)** at 15 ng/ml.

Annexin V/PI test was performed in order to evaluate the cell viability, while PI test was conducted to determine the effect of compound (**7)** on the cell cycle.

A double stain with Annexin V and PI was employed to determine the proportion of necrotic and apoptotic cells. PI stain normally label cells in late stage of apoptosis or necrosis, while annexin V labels early apoptotic cells [120, 121]. In comparison with the free CA4, the treatment with compound (**7)** demonstrated a significant increase in necrotic cells (around

50%) at the expense of the proportion of the apoptotic cells as the *p*-value was less than 0.05 (Figure 3.11).

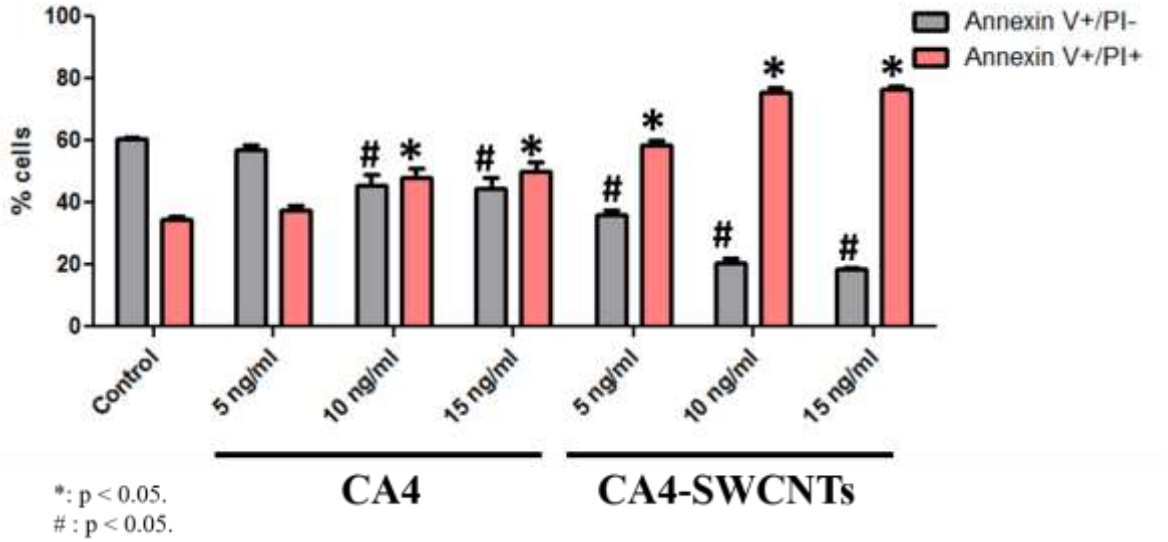

Figure 3.11: The Annexin V/ PI test for investigating the effect of different concentrations of CA4-SWCNTs and CA4 on cell necrosis and apoptosis after 48 hr incubation. Student t-test was applied.to compare the means. *P* value ≤ 0.05 was considered significant.

Moreover cell cycle PI test demonstrated that free CA4 and compound (**7)** caused G2/M arrest. However, with CA4 treatment higher proportion of cells were in the S-phase while greater proportion of cells appeared to be in the G1-phase after treatment with compound (**7)** (Figure 3.12). However, we believe that this does not necessarily mean that more cells were actually arrested in that phase. In fact, the principle of this flow cytometry assay is based on the ability of the PI stain to bind DNA in the nuclei. The more the cells have DNA the higher are the amount of the bound PI and consequently the stronger the signal detected by the flow cytometer. Apparently the cells treated with compound **(7)** were harmed by the treatment and the nuclei might become more leaky, and therefore more DNA might have been lost during the washing step which shifted the signal

form the region of S-phase to the region of G1 phase where it might have overlapped with the signal of the cells that are actually in G1-phase [122].

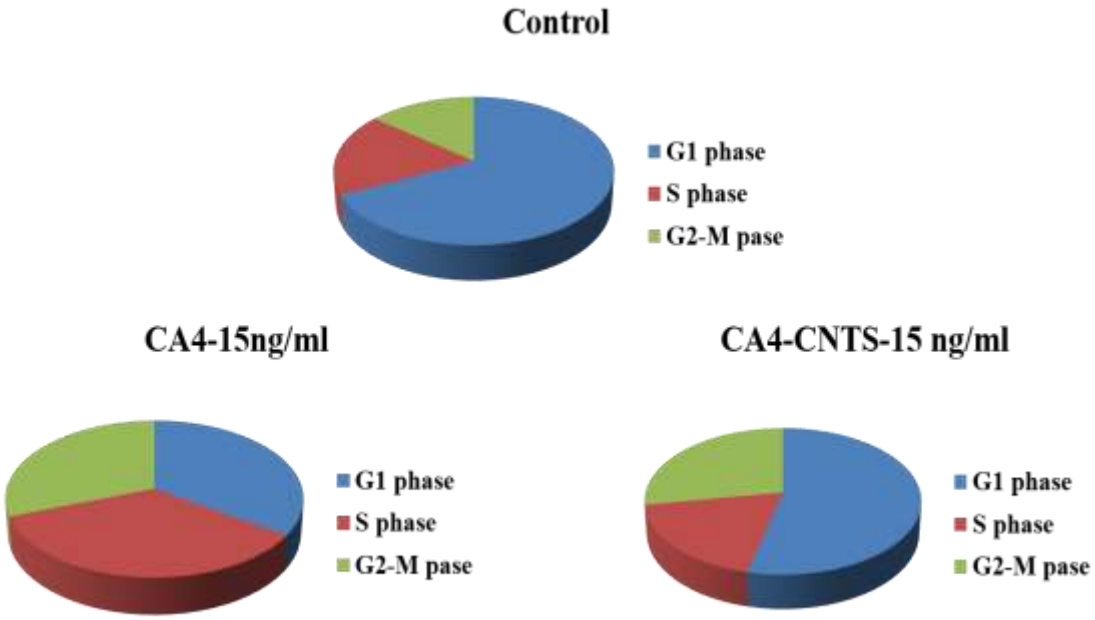

Figure 3.12: The cell cycle test of CA4-SWCNTs **(7)** and CA4 compared with cell without treatment (control)

Conclusion

Successful covalent functionalization of SWCNTs with CA4 has been realized. Moreover, dual functionalization has been achieved with the targeting agent, FA. The functionalization demonstrated good dispersibility of the functionalized SWCNTs as confirmed by TEM and SEM. The degree of functionalization was 45% and 50.4% for compound (**7)** and (**13)** respectively. The *in vitro* release profile showed more than 90% of the loaded CA4 was released within 48 hrs from the CA4-SWCNTs (**7)** at pH 7.4 and 37 ºC. Regarding the anticancer activity, the MTS proliferation assay showed that 15 ng/ml of the compound (**7)** is the most adequate concentration to provide a good anticancer activity with minimal cytotoxicity. Moreover, the annexin V/PI test demonstrated a significant increase in the necrotic cells (more than 50%) in comparison to the CA4 alone. The cell cycle PI test showed that both CA4 and compound (**7)** caused G2/M arrest. In conclusion, the developed nano anticancer drug system has the potential to improve the anticancer activity of CA4 and provide a novel therapy for cancer. The cytotoxic effect of compound **(13)** is still under investigation.

Limitation and suggestion for future work

The time which need to establish and prepare the cell culture lab and the lack of NMR, TEM, SEM, TGA were the main obstacles against our research activities.

Future work may include:

1) Study the anticancer activity of CA4-SWCNTs nano-system against different cancer cell lines.

2) Evaluate the cytotoxic effect of CA4-SWCNTs against normal cell lines.

3) Study the *in vitro* release profile of CA4 from CA4-FA-SWCNTs nano-system.

4) Determine the anticancer activity of CA4-FA-SWCNTs against cancer cells and define the importance of the targeting agent.

5) Conduct an *in vivo* experiments to examine the effectiveness of these nano-anticancer.

References

1. Jackson, A.L. and L.A. Loeb, **The contribution of endogenous sources of DNA damage to the multiple mutations in cancer.** Mutation Research/Fundamental and Molecular Mechanisms of Mutagenesis, 2001. **477**(1-2): p. 7-21.

2. education, p. *Cell cycle*, **control and the mitotic index**. [cited 2017 21-2]; Available from: https://www.philpoteducation.com/mod/book/view.php?id=779&chapterid=1123.

3. repropedia. **cancer.** 14.2.2017]; Available from: http://www.repropedia.org/cancer.

4.*http://cisncancer.org/research/what_we_know/advances/angiogenesis.html*.

5. DeBerardinis, R.J., et al., **The Biology of Cancer: Metabolic Reprogramming Fuels Cell Growth and Proliferation**. Cell Metabolism, 2008. **7**(1): p. 11-20.

6. Folkman, J., **What is the evidence that tumors are angiogenesis dependent?** CancerSpectrum Knowledge Environment, 1990. **82**(1): p. 4-6.

7. Kagan, V.E., et al., **Carbon nanotubes degraded by neutrophil myeloperoxidase induce less pulmonary inflammation**. Nature nanotechnology, 2010. **5**(5): p. 354-359.

8. Folkman, J., **Angiogenesis in cancer, vascular, rheumatoid and other disease.** Nature Medicine, 1995. **1**(1): p. 27-30.

9. Dvorak, H.F., et al., ***Identification and characterization of the blood vessels of solid tumors that are leaky to circulating macromolecules.*** **The American journal of pathology**, 1988. 133(1): p. 95.

10. Eberhard, A., et al., **Heterogeneity of angiogenesis and blood vessel maturation in human tumors: implications for antiangiogenic tumor therapies**. Cancer Research, 2000. **60**(5): p. 1388-1393.

11. Matsumura, Y. and H. Maeda, **A new concept for macromolecular therapeutics in cancer chemotherapy: mechanism of tumoritropic accumulation of proteins and the antitumor agent smancs**. Cancer Res, 1986. **46**(12 Pt 1): p. 6387-92.

12. Boucher, Y., L.T. Baxter, and R.K. Jain, **Interstitial pressure gradients in tissue-isolated and subcutaneous tumors: implications for therapy.** Cancer Research, 1990. **50**(15): p. 4478-4484.

13. Pawar, V.K., et al., ***Engineered nanocrystal technology: In-vivo fate, targeting and applications in drug delivery***. **Journal of Controlled Release**, 2014. **183**: p. 51-66.

14. Stewart, B. and C.P. Wild, **World cancer report 2014**. World, 2016.

15. Delaney, G., et al., **The role of radiotherapy in cancer treatment.** Cancer, 2005. **104**(6): p. 1129-1137.

16. Dougan, M. and G. Dranoff, **Immunotherapy of cancer, in Innate immune regulation and cancer immunotherapy.** 2012, Springer. p. 391-414.

17. Scott, A.M., J.D. Wolchok, and L.J. Old, **Antibody therapy of cancer.** Nature Reviews Cancer, 2012. **12**(4): p. 278-287.

18. Lindley, C., et al., **Perception of Chemotherapy Side Effects Cancer versus Noncancer Patients.** Cancer Practice, 1999. **7**(2): p. 59-65.

19. Jorio, A., G. Dresselhaus, and M.S. Dresselhaus, **Carbon nanotubes: advanced topics in the synthesis, structure, properties and applications.** Vol. 111. 2007: Springer Science & Business Media.

20. Cheng, L.-C., et al., **Nano–bio effects: interaction of nanomaterials with cells**. Nanoscale, 2013. **5**(9): p. 3547.

21. Iijima, S., **Helical Microtubules of Graphitic Carbon**. Nature, 1991. **354**(6348): p. 56-58.

22. Harris, P.J., **Carbon Nanotubes and Related Structures.** Cambridge University Press, Cambridge, 1991.

23. Dresselhaus, M.S., G. Dresselhaus, and P.C. Eklund, **Science of fullerenes and carbon nanotubes: their properties and applications.** 1996: Academic press.

24. Mcbride, W., **Synthesis of Carbon Nanotube by Chemical Vapor Deposition**. Undergraduate Degree Thesis, College of William and Marry in Virginia, Williamsburg, 2001.

25. Baughman, R.H., **Carbon Nanotubes--the Route Toward Applications**. Science, 2002. **297**(5582): p. 787-792.

26. Iijima, S. and T. Ichihashi, **Single-shell carbon nanotubes of 1-nm diameter**. Nature, 1993. **363**(6430): p. 603-605.

27. Dai, H., **Carbon Nanotubes: Synthesis, Integration, and Properties.** Accounts of chemical research, 2002. **35**(12): p. 1035-1044.

28. Collins, P.G. and P. Avouris, **Nanotubes for Electronics.** Scientific Americ**an**, 2000. **283**(6): p. 62-69.

29. Meo, M. and M. Rossi, **Prediction of Young's modulus of single wall carbon nanotubes by molecular-mechanics based finite element modelling.** Composites Science and Technology, 2006. **66**(11-12): p. 1597-1605.

30. Yu, M.-F., et al., **Tensile loading of ropes of single wall carbon nanotubes and their mechanical properties**. Physical review letters, 2000. **84**(24): p. 5552.

31. Bandaru, P.R., ***Electrical Properties and Applications of Carbon Nanotube Structures.*** **Journal of Nanoscience and Nanotechnology**, 2007. **7**(4): p. 1239-1267.

32. Star, A., et al., **Electronic Detection of Specific Protein Binding Using Nanotube FET Devices.** Nano Letters, 2003. **3**(4): p. 459-463.

33. Futaba, D.N., et al., *S***hape-engineerable and highly densely packed single-walled carbon nanotubes and their application as super-capacitor electrodes.** Nature Materials, 2006. **5**(12): p. 987-994.

34. Zhao, Y., G. Xing, and Z. Chai, *Nanotoxicology:* **Are carbon nanotubes safe?** Nature Nanotechnology, 2008. **3**(4): p. 191-192.

35. Liu, Z., et al., **Circulation and long-term fate of functionalized, biocompatible single-walled carbon nanotubes in mice probed by Raman spectroscopy**. Proceedings of the National Academy of Sciences, 2008. **105**(5): p. 1410-1415.

36. Pacurari, M., et al., **Raw Single-Wall Carbon Nanotubes Induce Oxidative Stress and Activate MAPKs, AP-1, NF-[kappa] B, and Akt in Normal and Malignant Human Mesothelial Cells**. Environmental health perspectives, 2008. **116**(9): p. 1211.

37. Guo, J., et al., **Biodistribution of functionalized multiwall carbon nanotubes in mice.** Nuclear Medicine and Biology, 2007. **34**(5): p. 579-583.

38. Boswell, A., et al., **PET Imaging of Soluble Yttrium-86-Labeled Carbon Nanotubes in Mice.** PLoS ONE, 2007. **2**(9): p. e907.

39. McDevitt, M.R., et al., ***Tumor Targeting with Antibody-Functionalized, Radiolabeled Carbon Nanotubes***. **Journal of Nuclear Medicine,** 2007. **48**(7): p. 1180-1189.

40. Podesta, J.E., et al., **Antitumor Activity and Prolonged Survival by Carbon-Nanotube-Mediated Therapeutic siRNA Silencing in a Human Lung Xenograft Model**. Small, 2009: p. NA-NA.

41. Al-Jamal, K.T., et al., **Functional motor recovery from brain ischemic insult by carbon nanotube-mediated siRNA silencing.** Proceedings of the National Academy of Sciences, 2011. **108**(27): p. 10952-10957.

42. Rao, C.N.R., et al., **Nanotubes.** ChemPhysChem, 2001. **2**(2): p. 78-105.

43. Gutsche, C., *S.* Reich, C. Thomsen, J. Maultzsch: **Carbon nanotubes, basic concepts and physical properties.** Colloid and Polymer Science, 2004. **282**(11): p. 1299-1299.

44. Bhattacharjee, A. and N.G. Biswas, **DENDRIMERS AS POTENTIAL TOOL FOR FORMULATION DEVELOPMENT OF NOVEL DRUG DELIVERY SYSTEM.**

45. Liu, Z., et al., **Carbon materials for drug delivery & cancer therapy.** Materials today, 2011. **14**(7): p. 316-323.

46. Debnath, S., et al., ***A Study of the Interaction between Single-Walled Carbon Nanotubes and Polycyclic Aromatic Hydrocarbons: Toward Structure−Property Relationships***. **The Journal of Physical Chemistry C**, 2008. **112**(28): p. 10418-10422.

47. Angelikopoulos, P., et al., ***Dispersing Individual Single-Wall Carbon Nanotubes in Aqueous Surfactant Solutions below the cmc***. **The Journal of Physical Chemistry** C, 2010. **114**(1): p. 2-9.

48. Gao, J., et al., **Selective Wrapping and Supramolecular Structures of Polyfluorene–Carbon Nanotube Hybrids**. ACS Nano, 2011. **5**(5): p. 3993-3999.

49. Zhao, Y.-L. and J.F. Stoddart, **Noncovalent Functionalization of Single-Walled Carbon Nanotubes**. Accounts of chemical research, 2009. **42**(8): p. 1161-1171.

50. Prencipe, G., et al., ***PEG Branched Polymer for Functionalization of Nanomaterials with Ultralong Blood Circulation.*** **Journal of the American Chemical Society**, 2009. **131**(13): p. 4783-4787.

51. Guldi, D.M., et al., ***Supramolecular Hybrids of [60]Fullerene and Single-Wall Carbon Nanotubes.*** **Chemistry - A European Journal**, 2006. **12**(15): p. 3975-3983.

52. Yang, K., L. Zhu, and B. Xing, **Adsorption of Polycyclic Aromatic Hydrocarbons by Carbon Nanomaterials**. Environmental Science & Technology, 2006. **40**(6): p. 1855-1861.

53. Assali, M., et al., **Non-covalent functionalization of carbon nanotubes with glycolipids: glyconanomaterials with specific lectin-affinity**. Soft Matter, 2009. **5**(5): p. 948.

54. Assali, M., et al., I**mproved non-covalent biofunctionalization of multi-walled carbon nanotubes using carbohydrate amphiphiles with a butterfly-like polyaromatic tail**. Nano research, 2010. **3**(11): p. 764-778.

55. Liu, J., **Fullerene Pipes**. Science, 1998. **280**(5367): p. 1253-1256.

56. Bahr, J.L., et al., ***Functionalization of Carbon Nanotubes by Electrochemical Reduction of Aryl Diazonium Salts: A Bucky Paper Electrode***. **Journal of the American Chemical Society**, 2001. **123**(27): p. 6536-6542.

57. Tagmatarchis, N. and M. Prato, **F*unctionalization of carbon nanotubes via 1,3-dipolar cycloadditions.*** J**ournal of Materials Chemistry,** 2004. **14**(4): p. 437.

58. Mooney, E., et al., **The electrical stimulation of carbon nanotubes to provide a cardiomimetic cue to MSCs**. Biomaterials, 2012. **33**(26): p. 6132-6139.

59. Haddon, R.C., **Carbon Nanotubes**. Accounts of chemical research, 2002. **35**(12): p. 997-997.

60. Chen, Z., et al., ***Soluble Ultra-Short Single-Walled Carbon Nanotubes.*** **Journal of the American Chemical Society**, 2006. **128**(32): p. 10568-10571.

61. He, P. and M.W. Urban, **Controlled Phospholipid Functionalization of Single-Walled Carbon Nanotubes**. Biomacromolecules, 2005. **6**(5): p. 2455-2457.

62. Balasubramanian, K. and M. Burghard, **Chemically Functionalized Carbon Nanotubes**. Small, 2005. **1**(2): p. 180-192.

63. Khabashesku, V.N., W.E. Billups, and J.L. Margrave, **Fluorination of Single-Wall Carbon Nanotubes and Subsequent Derivatization Reactions.** Accounts of chemical research, 2002. **35**(12): p. 1087-1095.

64. Schmitt-Sody, M., et al., **Neovascular targeting therapy: paclitaxel encapsulated in cationic liposomes improves antitumoral efficacy**. Clin Cancer Res, 2003. **9**(6): p. 2335-41.

65. Holzinger, M., et al., ***Functionalization of Single-Walled Carbon Nanotubes with (R-)Oxycarbonyl Nitrenes.*** **Journal of the American Chemical Society**, 2003. **125**(28): p. 8566-8580.

66. Prato, M., K. Kostarelos, and A. Bianco, **Functionalized Carbon Nanotubes in Drug Design and Discovery**. Accounts of chemical research, 2008. **41**(1): p. 60-68.

67. Pastorin, G., et al., **Double functionalisation of carbon nanotubes for multimodal drug delivery**. Chemical Communications, 2006(11): p. 1182.

68. Zhang, L., et al., **Diels–Alder addition to fluorinated single walled carbon nanotubes.** Chemical Communications, 2005(26): p. 3265.

69. Graupner, R., et al., ***Nucleophilic−Alkylation−Reoxidation: A Functionalization Sequence for Single-Wall Carbon Nanotubes***. **Journal of the American Chemical Society,** 2006. **128**(20): p. 6683-6689.

70. Price, B.K., J.L. Hudson, and J.M. Tour, ***Green Chemical Functionalization of Single-Walled Carbon Nanotubes in Ionic Liquids.*** **Journal of the American Chemical Society,** 2005. **127**(42): p. 14867-14870.

71. Doyle, C.D. and J.M. Tour, **Environmentally friendly functionalization of single walled carbon nanotubes in molten urea.** Carbon, 2009. **47**(14): p. 3215-3218.

72. Xu, Y., et al., **Microwave-induced electrophilic addition of single-walled carbon nanotubes with alkylhalides.** Applied Surface Science, 2008. **254**(8): p. 2431-2435.

73. Dyke, C.A. and J.M. Tour, ***Solvent-Free Functionalization of Carbon Nanotubes.*** **Journal of the American Chemical Society**, 2003. **125**(5): p. 1156-1157.

74. Pettit, G.R., et al., ***Isolation and structure of combretastatin.*** **Canadian Journal of Chemistry**, 1982. **60**(11): p. 1374-1376.

75. Gill, R., et al., *A* **Comprehensive Review on Combretastatin Analogues as Tubulin Binding Agents.** Current Organic Chemistry, 2014. **18**(19): p. 2462-2512.

76. McGown, A.T. and B.W. Fox, *S***tructural and biochemical comparison of the anti-mitotic agents colchicine, combretastatin A4 and amphethinile**. Anticancer Drug Des, 1989. **3**(4): p. 249-54.

77. Tozer, G.M., et al., ***The biology of the combretastatins as tumour vascular targeting agents.*** **International Journal of Experimental Pathology**, 2002. **83**(1): p. 21-38.

78. Monk, K.A., et al., **Design, synthesis, and biological evaluation of combretastatin nitrogen-containing derivatives as inhibitors of tubulin assembly and vascular disrupting agents**. Bioorganic & Medicinal Chemistry, 2006. **14**(9): p. 3231-3244.

79. Zheng, Y., *G* **Protein Control of Microtubule Assembly**. Annual Review of Cell and Developmental Biology, 2004. **20**(1): p. 867-894.

80. Bayless, K.J., ***Microtubule Depolymerization Rapidly Collapses Capillary Tube Networks in Vitro and Angiogenic Vessels in Vivo through the Small GTPase Rho.*** **Journal of Biological Chemistry**, 2004. **279**(12): p. 11686-11695.

81. Ahmed, B., et al., ***Vascular targeting effect of combretastatin A-4 phosphate dominates the inherent angiogenesis inhibitory activity.*** **International Journal of Cancer**, 2003. **105**(1): p. 20-25.

82. Lin, H.L., et al., ***Combretastatin A4-Induced Differential Cytotoxicity and Reduced Metastatic Ability by Inhibition of AKT Function in Human Gastric Cancer Cells***. **Journal of Pharmacology and Experimental Therapeutics,** 2007. **323**(1): p. 365-373.

83. Shen, C.-H., et al., ***Combretastatin A-4 inhibits cell growth and metastasis in bladder cancer cells and retards tumour growth in a murine orthotopic bladder tumour model.*** **British Journal of Pharmacology,** 2010. **160**(8): p. 2008-2027.

84. Granata, R., L. Locati, and L. Licitra, **Therapeutic strategies in the management of patients with metastatic anaplastic thyroid cancer**. Current Opinion in Oncology, 2013: p. 1.

85. Pollock, J.K., et al., **Combretastatin (CA)-4 and its novel analogue CA-432 impair T-cell migration through the Rho/ROCK signalling pathway.** Biochemical Pharmacology, 2014. **92**(4): p. 544-557.

86. Lin, C.M., et al., *I***nteractions of tubulin with potent natural and synthetic analogs of the antimitotic agent combretastatin: a structure-activity study.** Molecular pharmacology, 1988. **34**(2): p. 200-208.

87. Gaukroger, K., et al., ***Novel Syntheses of Cis and Trans Isomers of Combretastatin A-4.*** **The Journal of Organic Chemistry,** 2001. **66**(24): p. 8135-8138.

88. Solladié, G., Y. Pasturel-Jacopé, and J. Maignan, **A re-investigation of resveratrol synthesis by Perkins reaction. Application to the synthesis of aryl cinnamic acids**. Tetrahedron, 2003. **59**(18): p. 3315-3321.

89. Cushman, M., et al., ***Synthesis and evaluation of stilbene and dihydrostilbene derivatives as potential anticancer agents that inhibit tubulin polymerization.*** **Journal of Medicinal Chemistry**, 1991. **34**(8): p. 2579-2588.

90. Schobert, R., K. Effenberger-Neidnicht, and B. Biersack, ***Stable combretastatin A-4 analogues with sub-nanomolar efficacy against chemoresistant HT-29 cells.*** **Int J Clin Pharmacol Ther**, 2011. **49**(1): p. 71-2.

91. Dark, G.G., et al., **Combretastatin A-4, an agent that displays potent and selective toxicity toward tumor vasculature**. Cancer Res, 1997. **57**(10): p. 1829-1834.

92. Young, S.L. and D.J. Chaplin, **Combretastatin A4 phosphate: background and current clinical status.** Expert Opinion on Investigational Drugs, 2005. **13**(9): p. 1171-1182.

93. Rustin, G.J.S., ***Phase I Clinical Trial of Weekly Combretastatin A4 Phosphate: Clinical and Pharmacokinetic Results.*** **Journal of Clinical Oncology,** 2003. **21**(15): p. 2815-2822.

94. Zweifel, M., et al., **Phase II trial of combretastatin A4 phosphate, carboplatin, and paclitaxel in patients with platinum-resistant ovarian cancer.** Annals of Oncology, 2011. **22**(9): p. 2036-2041.

95. Woods, J.A., et al., ***The interaction with tubulin of a series of stilbenes based on combretastatin A-4.*** **Br J Cancer,** 1995. **71**(4): p. 705-11.

96. Tozer, G.M., et al., **Combretastatin A-4 phosphate as a tumor vascular-targeting agent: early effects in tumors and normal tissues.** Cancer Res, 1999. **59**(7): p. 1626-34.

97. von Pawel, J., et al., **DISRUPT: A randomised phase 2 trial of ombrabulin (AVE8062) plus a taxane–platinum regimen as first-line therapy for metastatic non-small cell lung cancer.** Lung Cancer, 2014. **85**(2): p. 224-229.

98. ; Available from: http://adisinsight.springer.com/drugs/800011200.

99. **National Center for Biotechnology Information. PubChem Compound Database;** *CID=6918405*. [cited 2017 June 10]; Available from: https://pubchem.ncbi.nlm.nih.gov/compound/6918405.

100. Zhang, Y.-f., et al., ***Targeted delivery of RGD-modified liposomes encapsulating both combretastatin A-4 and doxorubicin for tumor therapy: In vitro and in vivo studies.*** **European Journal of Pharmaceutics and Biopharmaceutics**, 2010. **74**(3): p. 467-473.

101. Nallamothu, R., et al., **A tumor vasculature targeted liposome delivery system for combretastatin A4: Design, characterization, and in vitro evaluation.** AAPS PharmSciTech, 2006. **7**(2): p. E7-E16.

102. Wang, Z., W.-K. Chui, and P.C. Ho, **Nanoparticulate Delivery System Targeted to Tumor Neovasculature for Combined Anticancer and Antiangiogenesis Therapy**. Pharmaceutical Research, 2010. **28**(3): p. 585-596.

103. Falciani, C., et al., **Design and In vitro Evaluation of Branched Peptide Conjugates: Turning Nonspecific Cytotoxic Drugs into Tumor-Selective Agents**. ChemMedChem, 2010. **5**(4): p. 567-574.

104. Toffoli, G., et al., ***Overexpression of folate binding protein in ovarian cancers.*** **International Journal of Cancer**, 1997. **74**(2): p. 193-198.

105. Sudimack, J. and R.J. Lee, **Targeted drug delivery via the folate receptor.** Advanced Drug Delivery Reviews, 2000. **41**(2): p. 147-162.

106. Shi, X., et al., ***Multifunctional dendrimer/combretastatin A4 inclusion complexes enable in vitro targeted cancer therapy.*** **International Journal of Nanomedicine**, 2011: p. 2337.

107. Yang, T., et al., **Targeted delivery of a combination therapy consisting of combretastatin A4 and low-dose doxorubicin against tumor neovasculature**. Nanomedicine: Nanotechnology, Biology and Medicine, 2012. **8**(1): p. 81-92.

108. Wang, Y., et al., **pH-sensitive pullulan-based nanoparticle carrier of methotrexate and combretastatin A4 for the combination therapy against hepatocellular carcinoma**. Biomaterials, 2013. **34**(29): p. 7181-7190.

109. Su, T., et al., ***Construction of a two-in-one liposomal system (TWOLips) for tumor-targeted combination therapy***. **International Journal of Pharmaceutics**, 2014. **476**(1-2): p. 241-252.

110. Sumer Bolu, B., E. Manavoglu Gecici, and R. Sanyal, **Combretastatin A-4 Conjugated Antiangiogenic Micellar Drug Delivery Systems Using Dendron–Polymer Conjugates.** Molecular Pharmaceutics, 2016. **13**(5): p. 1482-1490.

111. Ding, F., et al., **A tumor-targeting drug delivery system based on cyclic NGR-modified, combretastatin A4-loaded, functionalized graphene oxide nanosheets**. RSC Adv., 2016. **6**(72): p. 68134-68140.

112. Assali, M., et al., **Synthesis and non-covalent functionalization of carbon nanotubes rings: new nanomaterials with lectin affinity.** Nanotechnology, 2013. **24**(8): p. 085604.

113. Xiao, C.-F., et al., **Hydroxyl Substitutional Effect on Selective Synthesis ofcis, transStilbenes and 3-Arylcoumarins Through Perkin Condensation.** Synthetic Communications, 2012. **42**(9): p. 1243-1258.

114. Ménard-Moyon, C., et al., ***One-Pot Triple Functionalization of Carbon Nanotubes.*** **Chemistry-A European Journal,** 2011. **17**(11): p. 3222-3227.

115. Sarin, V.K., et al., **Quantitative monitoring of solid-phase peptide synthesis by the ninhydrin reaction.** Analytical biochemistry, 1981. **117**(1): p. 147-157.

116. Dulbecco, R. and M. Vogt, ***Plaque formation and isolation of pure lines with poliomyelitis viruses***. **The Journal of experimental medicine,** 1954. **99**(2): p. 167-182.

117. J. Sambrook, E.F.F.a.T.M., **Molecular Cloning: A Laboratory Manual.** 1989, Cold Spring Harbor Laboratory Press, Cold Spring Harbor: New York.

118. Wen, S., et al., **Targeted and pH-Responsive Delivery of Doxorubicin to Cancer Cells Using Multifunctional Dendrimer-Modified Multi-Walled Carbon Nanotubes.** Advanced Healthcare Materials, 2013. **2**(9): p. 1267-1276.

119. Kaiser, E., et al., **Color test for detection of free terminal amino groups in the solid-phase synthesis of peptides.** Analytical biochemistry, 1970. **34**(2): p. 595-598.

120. Vermes, I., et al., ***A novel assay for apoptosis Flow cytometric detection of phosphatidylserine expression on early apoptotic cells using fluorescein labelled Annexin V.*** **Journal of Immunological Methods**, 1995. **184**(1): p. 39-51.

121. Vermes, I., C. Haanen, and C. Reutelingsperger, ***Flow cytometry of apoptotic cell death.*** **Journal of Immunological Methods**, 2000. **243** (1-2): p. 167-190.

122. Kanthou, C., et al., ***The Tubulin-Binding Agent Combretastatin A-4-Phosphate Arrests Endothelial Cells in Mitosis and Induces Mitotic Cell Death.*** **The American journal of pathology**, 2004. **165**(4): p. 1401-1411.

جامعة النجاح الوطنية

كلية الدراسات العليا

التفعيل البيولوجي لأنابيب الكربون النانونية بمركب كومبريتاستاتين أ4 لعلاج السرطان بطريقة مستهدفة

إعداد

ديمه فهيم " محمد رشدي" حمد

إشراف

د. محي الدين العسالي

أ. د.عبد الناصر زيد

قدمت هذه الأطروحة استكمالاً لمتطلبات الحصول على درجة الماجستير في العلوم الصيدلانية بكلية الدراسات العليا في جامعة النجاح الوطنية في نابلس- فلسطين.

2017

التفعيل البيولوجي لأنابيب الكربون النانونية بمركب كومبريتاستاتين أ4 لعلاج السرطان بطريقة مستهدفة

إعداد

ديمه فهيم " محمد رشدي" حمد

إشراف

د. محي الدين العسالي

أ. د. عبد الناصر زيد

الملخص

يعتبر العلاج الكيماوي هو الدعامة الأساسية لعلاج مرض السرطان. لكن لسوء الحظ، العلاج الكيماوي يمكن أن يؤثر ليس فقط على الخلايا السرطانية ولكن أيضاعلى الخلايا الصحية مسبباً آثار جانبية عديدة.وبالتالي العديد من الباحثين حريصون على تطوير أنظمة توصيل جديدة للدواءالتي قد تساعد من ناحية على تقليل الجرعات المستخدمة من العلاج الكيماوي، ومن ناحية أخرى توصيل العلاج الكيميائي للخلايا السرطانية بشكل مستهدف.واحدة من أنظمة توصيل الدواء الحديثة في هذا المجال هي تكنولوجياأنابيب الكربون النانونية.

الهدفالاساسي لهذه الاطروحة هو التفعيل التساهمي للأنابيب الكربون النانونية وربطها بالعديد من جزيئات الكومبريتاستاتين أ4 المضاد السرطان عند طريق استخدام تفاعل كليك وذلك للحصول على دواء نانوني بدرجة عالية من الثبات بوجود رابط مشتق من رباعي إيثيلين غليكول لتحسين ذائبيتها. بالاضافة الى ذلك، ومن أجل استهداف الخلايا السرطانية خصيصا، تم تحميل عامل الاستهداف حمض الفوليك على النظام النانوي. ولقد أظهر تحليل الدواء النانوني بواسطة المجهر الالكتروني النافذ والمجهر الالكتروني الماسح تفرق وتوزع جيد للانابيب النانونية بقطريتراوح بين (5–15) نانومتر. بالاضافة الى ذلك، تم تحديد كفاءة التفعيل لانابيب الكربون النانونية بواسطة جهاز التحليل الحراري الذي أظهر بنسبة 45% لأنابيب الكربونية المحملة بالكومبريتاستانين أ4 وبنسبة 50% لأنابيب الكربونية المحملة بالكومبريتاستانين أ4–حمض الفوليك.

وأظهرت دراسة نمط خروج دواء الكومبريتاستاتين أ4 من الانابيب النانونية أن أكثر من٩٠٪ من الدواء تم خروجه خلال 50 ساعة على درجة الحموضة 7.4 و 37 درجة مئوية.

أما فيما يخص النشاط المضاد للسرطان، تم تنفيذ اختبار التكاثر لخلايا السرطان ال م.ت.س وتم تحديد التركيز المناسب من الأنابيب الكربونية المحملة بالكومبريتاستانين أ4 هو 15 نانوغرام\مل. بعد ذلك تم تقييم النشاط السمي للخلايا لهذا الدواء النانوي عن طريقجهاز قياس التدفق الخلوي باستخدام إختباري الأنيكسين 5/ يوديد البروبيديوم. بالمقارنة مع الكومبريتاستاتين أ4، فأن الأنابيب الكربونية المحملة بالكومبريتاستانين أ4 أظهرت زيادة نسبة الخلايا المنخورة بحوالي 50% على حساب الخلايا الميتة بشكل مبرمج. بالإضافة الى ذلك، فإن أختبار دورة حياة الخلية أظهر أن الكومريتاستانين أ4 والأنابيب الكربونية المحملة بالكومبريتاستانين أ4 تسببت بأيقاف انقسام الخلايا عند مرحلة (G2\M) . لكن مع علاج الكومبريتاستاتين أ4 فإن هناك نسبة أكبر من الخلايا في مرحلة (S–phase) بينما مع الأنابيب الكربونية المحملة بالكومبريتاستانين أ4فإن هناك نسبة أكبر من الخلايا في مرحلة (G1–phase). مع البيانات المقدمة مجتمعة معا فان الأنابيب الكربونية المحملة بالكومبريتاستانين أ4 لها فعالية ملحوظة وكبيرة ضد السرطان والتي قد تكونمتفوقة على الكومبريتاستاتين أ4 .اما بالنسبة للنشاط المضاد للسرطان للأنابيب الكربونية المحملة بالكومبريتاستانين أ4–حمض الفوليك فأنه تحت الدراسة.